Monthly Notices of the ROYAL ASTRONOMICAL SOCIETY

MNRAS **506,** 4715–4734 (2021) https://doi.org/10.1093/mnras/stab1938
Advance Access publication 2021 July 8

A systematic reclassification of Type IIn supernovae

C. L. Ransome [1]★ S. M. Habergham-Mawson,[1] M. J. Darnley [1] P. A. James,[1] A. V. Filippenko[2,3] and E. M. Schlegel[4]

[1]*Astrophysics Research Institute, Liverpool John Moores University, Liverpool Science Park iC2, 146 Brownlow Hill, Liverpool, Merseyside L3 5RF, UK*
[2]*Department of Astronomy, University of California, Berkeley, CA 94720-3411, USA*
[3]*Miller Institute for Basic Research in Science, University of California, Berkeley, CA 94720, USA*
[4]*Department of Physics and Astronomy, University of Texas at San Antonio, One UTSA Circle, San Antonio, TX 78249, USA*

Accepted 2021 July 2. Received 2021 June 2; in original form 2021 March 17

ABSTRACT

Type IIn supernovae (SNe IIn) are a relatively infrequently observed subclass of SNe whose photometric and spectroscopic properties are varied. A common thread among SNe IIn is the complex multiple-component hydrogen Balmer lines. Owing to the heterogeneity of SNe IIn, online data bases contain some outdated, erroneous, or even contradictory classifications. SN IIn classification is further complicated by SN 'impostors' and contamination from underlying H II regions. We have compiled a catalogue of systematically classified nearby (redshift $z < 0.02$) SNe IIn using the Open Supernova Catalogue (OSC). We present spectral classifications for 115 objects previously classified as SNe IIn. Our classification is based on results obtained by fitting multiple Gaussians to the H α profiles. We compare classifications reported by the OSC and Transient Name Server (TNS) along with the best matched templates from SNID. We find that 28 objects have been misclassified as SNe IIn. TNS and OSC can be unreliable; they disagree on the classifications of 51 of the objects and contain a number of erroneous classifications. Furthermore, OSC and TNS hold misclassifications for 34 and 12 (respectively) of the transients we classify as SNe IIn. In total, we classify 87 SNe IIn. We highlight the importance of ensuring that online data bases remain up to date when new or even contemporaneous data become available. Our work shows the great range of spectral properties and features that SNe IIn exhibit, which may be linked to multiple progenitor channels and environment diversity. We set out a classification scheme for SNe IIn based on the H α profile that is not greatly affected by the inhomogeneity of SNe IIn.

Key words: line: profiles – techniques: spectroscopic – catalogues – circumstellar matter – stars: winds, outflows – transients: supernovae.

1 INTRODUCTION

Type IIn supernovae (SNe IIn) are a somewhat uncommon subclass of SNe accounting for around 7 per cent of detected core-collapse SNe (CCSNe; Li et al. 2011). Schlegel (1990) analysed optical spectra of Type II SNe and noticed that three of the spectra (SN 1987F, SN 1988Z, and SN 1989C) exhibited relatively narrow features superimposed on the broader hydrogen Balmer emission lines. Those three objects had a very blue continuum and lacked the P Cygni profiles one would associate with a normal SN II. These so-called SNe IIn (with the 'n' denoting the narrow features) are characterized by multicomponent Balmer line profiles with the most obvious example being the H α line. One may observe a relatively narrow feature with a full width at half-maximum (FWHM) intensity of the order of hundreds of km s^{-1} (and sometimes also an even narrower, unresolved feature), an intermediate feature a few thousands of km s^{-1} wide, and a broad component up to tens of thousands of km s^{-1} wide (Filippenko 1997). SN 1988Z is often used as a prototype SN IIn and may be used as a subtype of SNe IIn (other notable SNe IIn, such as the well-studied SN 1998S, are also used as subtypes).

The mechanism that drives the formation of the narrow H features is the SN ejecta shocking a pre-existing, cold, slow, and dense circumstellar medium (CSM). Emission from the initial interaction then ionizes the surrounding unshocked CSM, resulting in an H α excess (Chugai 1991; Chugai et al. 2004). The broad components of the lines originate from the fast-moving SN ejecta. The intermediate components may form from the SN ejecta interacting with a dense, clumpy wind (Chugai et al. 2004), broadened by the scattering of photons from thermal electrons (Chugai 2001; Dessart et al. 2009; Humphreys et al. 2012; Huang & Chevalier 2018), or from the dense, shocked shell (Kiewe et al. 2012). These features can constitute the classic SN IIn H α profile shape, reminiscent of the Eiffel Tower, as can be seen in Fig. 1 that shows an example model H α profile constructed from three Gaussian components (with FWHM $\approx$ 200, 1100, and 2700 km s^{-1}).

There are several possible origins for this pre-existing CSM. It has been proposed that the progenitor systems of SNe IIn undergo mass-loss episodes preceding their terminal SN explosion (Smith 2014). Using light-curve modelling analysis on the bolometric light curves of a sample of SNe IIn, Moriya et al. (2014) found that the mass-loss rate of many SN IIn progenitors exceeds 10^{-3} M$_\odot$ yr^{-1}.

★ E-mail: C.Ransome@2018.ljmu.ac.uk

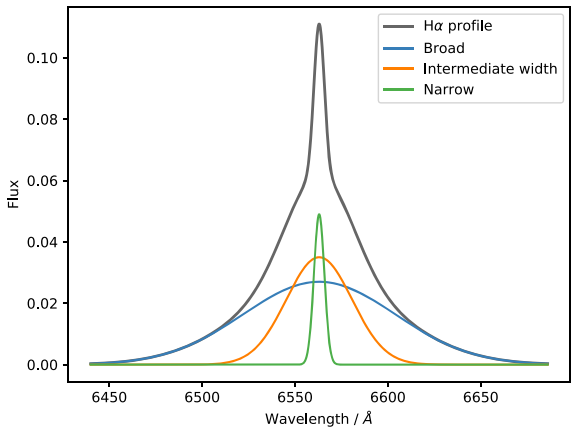

Figure 1. An example SN IIn H α profile with the narrow, intermediate-width, and broad components shown. This is an example of the classic SN IIn 'Eiffel Tower' shape that is the product of three model Gaussian components.

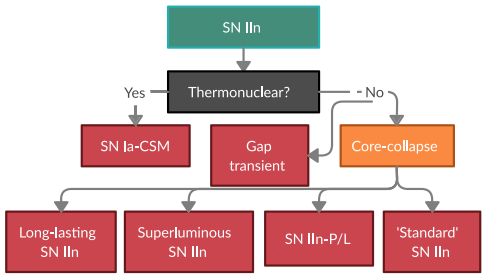

Figure 2. A breakdown of the routes an SN IIn can take based on the nature of the explosion and other observed spectroscopic and photometric properties.

Some SNe IIn undergo significant mass-loss episodes in the years preceding the SN explosion (Ofek et al. 2014). SN 2009ip was initially recognized as an 'SN impostor' (see Section 1.1.3) at its 2009 eruption, and then in 2012 it evolved into an SN IIn following its terminal explosion or a period of eruptive mass-loss from its luminous blue variable (LBV) progenitor (see Section 1.1.1; Mauerhan et al. 2013; Ofek et al. 2014; Pastorello et al. 2017). This latter mode of mass-loss was also observed in SN 2015bh (Boian & Groh 2018), SN 2016bdu (Pastorello et al. 2017), and SN 2018cnf (Pastorello et al. 2019b).

SNe IIn are observationally very diverse. There is a wide luminosity range, with some SNe IIn inhabiting the standard CCSN space in the luminosity–time-scale phase-space diagram (Kasliwal 2011) at peak absolute magnitudes around −17 to −19 (Li et al. 2011; Kiewe et al. 2012; Taddia et al. 2013). Some SNe IIn, such as SN 2006gy, reach −22 mag (the most luminous SN observed at the time; Smith et al. 2007). This may be considered as a superluminous SN IIn (SLSN-IIn). Using light-curve modelling, Moriya et al. (2012) found that the CSM shell contained around 15 $M_{\odot}$ of H-rich material and the SN ejecta contained similar mass. The light curve of SN 2006gy is also very long lived, lasting ∼3000 d (Fox et al. 2015). A further example of long-lasting SN IIn emission is SN 2005ip, which remained the brightest H α source in its host galaxy (NGC 2906) for several years (Stritzinger et al. 2012; Smith et al. 2017) with a decline only recently (Fox et al. 2020). Smith et al. (2017) find that such long-lived emission from SNe IIn requires mass-loss episodes from the SN progenitor to occur for 1000 yr preceding the explosion. Some SNe IIn also show signs of pre-existing dust in the CSM shell revealed through infrared (IR) observations (e.g. SN 2010jl, Bevan et al. 2020; SN 2014ab, Moriya et al. 2020; SN 2017hcc, Smith & Andrews 2020). Other transients show CSM interaction for a brief period, perhaps indicating a more confined CSM (e.g. SN 2008fq, Taddia et al. 2013; SN 2018zd, Zhang et al. 2020). Some SNe IIn follow the standard light-curve decay time-scale for CCSNe of a few hundred days and Nyholm et al. (2020) found that there were two populations of SNe IIn in terms of light-curve rise times, with fast risers and slow risers. In other cases, the light-curve shape is that of a Type IIP SN with a plateau phase that may be due to the inward recombination front and the outward expansion of the SN ejecta. These two processes occur at a similar rate, resulting in the brightness of the object being almost constant. The light-curve shape may resemble that of a Type IIL SN, where the light curve drops off linearly (in magnitudes) with time, owing to the progenitor star having a smaller H-rich envelope following greater mass-loss (e.g. SN 2011ht, SN IIP-like, Mauerhan et al. 2013; Bullivant et al. 2018, SN 2013fs, SN IIP-like, and SN 2013fr, SN IIL-like). However, as more SNe are observed, the clear distinction between light-curve morphologies is blurred, and there may be a continuum of light-curve shapes rather than a larger number of discrete categories. Anderson et al. (2014) investigated the diversity in the *V*-band light curves of 116 SNe II and found a continuum between lower luminosity events with a plateau in the light curve and brighter events with a linear, more rapid decline (see also Hamuy 2003; Sanders et al. 2015; Valenti et al. 2016). The possible subtypes of SNe IIn are outlined in Fig. 2.

Along with this photometric diversity, we note that there are accompanying differences in the spectra of SNe IIn. Generally speaking, one may expect to see lines of O I, He I, Ca II, and Fe II along with H I emission. However, the common defining traits are the multicomponent H α lines with the signature narrow features (see Fig. 1) and a blue continuum. However, even these H α profiles can be diverse in strength, duration, and shape. Some SNe IIn exhibit their narrow features and multicomponent H α (and other Balmer line) profiles throughout their evolution. Other SNe IIn seem to show narrow features only in the early stages of their evolution, with these features lasting just a few days or even hours. Ofek et al. (2014) term such transients with short-lived SN IIn phases as 'weak' SNe IIn, with an example being PTF11iqb (Smith et al. 2015). These 'weak' SNe IIn may suggest that lower mass SN progenitors experience the mass-loss required for the CSM interaction as seen in some SNe IIP and SNe IIL (for example, ASASSN-15oz, Bostroem et al. 2019; SN 2013fs and SN 2013fr, Bullivant et al. 2018). While SNe IIn do not typically show the broad P Cygni features one observes in other SNe II, we do sometimes see narrow P Cygni absorption associated with the narrow H α features. Moreover, asymmetry in both the SN ejecta and the surrounding CSM can profoundly affect the shape of the H α profile. In some cases, we observe SNe IIn exploding within an aspherical and/or clumpy CSM where one may see asymmetric redshifted or blueshifted components in the H α profiles (for example, there may be blueshifted wings in the later epochs of the spectra of SN 2008J; see Fig. 4). In the case of an SN IIn having an LBV progenitor (see Section 1.1.1), we can easily infer how this asymmetry and complex structure (e.g. SN 1998S; Mauerhan & Smith 2012; Shivvers et al. 2015) can arise by observing the Homunculus nebula around the LBV η Carinae with its asymmetric lobes (Smith et al. 2003; Smith 2006; Akashi & Kashi 2020; Kurfürst, Pejcha & Krtička 2020; Millour et al. 2020). When one considers the viewing angle to the observer, it is clear that CSM geometry is important to our observations as the results of this asymmetry are a deviation from the classic SN IIn H α profile shape.

1.1 Possible progenitor systems of SNe IIn

1.1.1 LBVs

LBVs arise from massive stars undergoing a transition phase from an O-type star to a Wolf–Rayet (WR) star where the outer H-rich layer has been expelled (Humphreys & Davidson 1994; Weis & Bomans 2020). LBVs are characterized by mass-loss through winds at a rate of up to $\sim 10^{-4}\,M_{\odot}\,yr^{-1}$ (Vink 2018) and also episodic eruptions. The mass-loss from these eruptive episodes (for example, the great eruption of η Car) can reach up to $10\,M_{\odot}$ with $\dot{M} \approx 1\,M_{\odot}\,yr^{-1}$ (Smith et al. 2003, 2010). The H-rich CSM that surrounds SNe IIn may originate from the material ejected in these dramatic mass-shedding events (see Smith 2014, and references therein). Notable examples of the LBV class include P Cygni (Smith & Hartigan 2006) and η Car (Smith et al. 2003) in the Milky Way and S Doradus in the Small Magellanic Cloud (Smith & Tombleson 2015). These mass-loss periods of LBVs correspond to increases in the luminosity of the star. Ofek et al. (2014) found that around half of SN IIn progenitor systems experience such brightening at least 120 d before the final terminal SN explosion. According to Gal-Yam et al. (2007), archival data show that SN 2005gl in NGC 266 had an LBV progenitor. Gal-Yam & Leonard (2009) found that the LBV progenitor had a mass that exceeded $50\,M_{\odot}$. This was the first confirmed LBV progenitor system for an SN IIn.

As LBVs are high-mass stars, they are expected to reside in young environments close to O-type stars. However, Smith & Tombleson (2015) found that many LBVs are isolated from any cluster of O-stars. The authors propose a scenario where a WR star is a mass donor in an interacting binary system with an LBV mass gainer. Through these interactions, the LBV may be kicked out of its place of birth, leading to the observed isolation. This is consistent with the findings of Habergham et al. (2014) described in Section 1.2: Many SNe IIn reside in environments devoid of star formation (SF). Another route for LBV formation is through binary mergers that may account for their apparent isolation (Justham, Podsiadlowski & Vink 2014; Aghakhanloo et al. 2017).

1.1.2 Yellow hypergiants

Yellow hypergiants (YHGs) are evolved post-red-supergiant (RSG) stars with $M_{\rm ZAMS} \approx 20$–$60\,M_{\odot}$ that undergo enhanced mass-loss that may form the required CSM for the SN IIn phenomenon (for a review, see de Jager 1998). Brennan et al. (2021a,b) present a detailed analysis of the SN IIn candidate AT 2016jbu, which was found to be an SN 2009ip-like object with a double-peaked light curve and a dusty circumstellar shell. Using archival *Hubble Space Telescope* (*HST*) imaging, the authors found that the progenitor of AT 2016jbu was consistent with a YHG of $M \approx 20\,M_{\odot}$. With age estimates of the possible progenitor of AT 2016jbu and the age of the environment of the transient, a CCSN scenario was favoured over a non-terminal explosion while an 'impostor' event could not be ruled out.

1.1.3 Gap transients and supernova impostors

Some transients are initially classified as SNe IIn because they exhibit the multicomponent and narrow H α emission features. However, it later becomes apparent, when the progenitor star is reobserved after the brightening phase, that some events originate from non-terminal explosions within dense CSM. These transients typically lie within gaps in the time-scale–luminosity phase space of exploding transients (Kasliwal 2011). With absolute magnitudes ranging from -10 to -14 (between novae and SNe), they may be generally termed 'gap transients'. A subset of them is sometimes named SN 'impostors'; they have spectra similar to those of SNe IIn, but they are subluminous, typically $M_V \approx (-11)$–(-14) (Kochanek, Szczygieł & Stanek 2012). Such events may be due to mass-loss episodes from LBVs, similar to the great eruption of η Car (Smith et al. 2011). After this initial eruption, the progenitor may be obscured by dust that forms after the initial eruption (Kochanek et al. 2012); however, some objects such as SN 2002kg do not much dust (Kochanek et al. 2012; Humphreys et al. 2014, 2017). Other examples that appear in this work include SN 1997bs, SN 1999bw, SN 2000ch, SN 2001ac, and SN 2002kg (Kochanek et al. 2012). These outbursts can sometimes precede a possible full SN explosion – for example, SN 2006jc (an SN Ibn rather than an SN IIn; Pastorello et al. 2007; Smith et al. 2013), SN 2009ip (Foley et al. 2011; Mauerhan et al. 2013; Pastorello et al. 2013), and SN 2015bh (Thöne et al. 2017; Boian & Groh 2018).

In some cases, such as SN 2009ip, the nature of the 'final' eruption is debated. Pastorello et al. (2013) and Smith, Mauerhan & Prieto (2014) noted that the high luminosity of the 'final' eruption (~ -18 mag) of SN 2009ip and its broad, persistent emission features suggested a large ejecta mass and explosion energy (around 10^{51} erg), pointing towards a terminal CCSN explosion. However, the CCSN scenario is disputed; Fraser et al. (2013) found that the spectrum of SN 2009ip in 2012 December resembled the one after the initial 2009 eruption. Furthermore, they found no evidence of nucleosynthesized elements, and the peak luminosity could be achieved by considering efficient kinetic-energy transfer from the ejecta colliding with CSM from eruptive LBV mass-loss episodes, suggesting a non-terminal scenario for SN 2009ip. Fraser et al. (2015) found that by 2014 December, SN 2009ip had not yet dimmed below the level of the pre-discovery images and still had not entered the nebular phase expected in CCSNe. This may suggest a non-terminal explosion mechanism, but the authors do not rule out continuing CSM interaction after core collapse being responsible for these features. Elias-Rosa et al. (2018) found that SN Hunt151 was remarkably similar to the eruption of SN 2009ip; they suggested that SN Hunt151 may be an η Car-like LBV eruption within a dense CSM cocoon.

Other notable 'impostors' include SN 2008S (the namesake for a group of similar objects; Thompson et al. 2009) in NGC 6946 (Arbour 2008), where a progenitor was unable to be recovered. Prieto et al. (2008) reported that the culprit may have been a lower mass ($\sim 10\,M_{\odot}$) star in a dusty environment; hence, this object could be an enshrouded 'impostor'. Kochanek (2011) argued that SN 2008S and the similar transient NGC 300-OT are consistent with an explosion taking place in an environment with very dusty winds. Berger et al. (2009a) found that the progenitor of NGC 300-OT may be a compact object such as a WR star or blue supergiant (BSG), contrary to the RSG interpretation of Kochanek (2011). Andrews et al. (2020) suggested that the progenitor of the SN 2008S-like transient AT 2019krl is a BSG/LBV, based on archival *HST*, *Spitzer Space Telescope*, and Large Binocular Telescope data. They also discussed the possibility that the transient was caused by binary interaction in the form of a merger that resembled an LBV eruption (briefly discussed in Section 1.1.1, but see also Smith et al. 2016, 2018). An alternative scenario to the LBV/BSG and non-terminal path (Berger, Foley & Ivans 2009b; Bond et al. 2009; Smith et al. 2009; Kochanek 2011; Andrews et al. 2020) for SN 2008S-like transients may be RSG/super-AGB (asymptotic giant branch) progenitors that suffer terminal electron-capture supernova (ecSN) explosions, discussed in Section 1.1.4. Botticella et al. (2009) found that the bolometric light curve of SN 2008S was consistent with the decay of ^{56}Co and

suggested that the progenitor was a super-AGB star with $M \approx (-6)$–$(-8)\,M_{\odot}$ that ended its life as an ecSN. Adams et al. (2016) reported that SN 2008S had become fainter than its progenitor, arguing that the explosion was terminal. The dusty environments of SN 2008S-like transients complicate attempts to detect a surviving progenitor; as such, the nature of these objects remains elusive.

While SN 'impostors' are subluminous, there may still be luminosity overlap with some genuine SNe such as SNe IIn-P and SNe that are obscured by dust – as in the aforementioned terminal scenario for SN 2008S-like transients. The outbursts of SN 2009ip reached absolute magnitudes of −15 and −18 (Smith et al. 2013); if the final 2012 event was not terminal, then SN impostors driven by CSM interaction may overlap most of the luminosity space of SNe. Therefore, distinguishing between 'impostor' events and genuine SNe can be difficult without late-time imaging showing the surviving progenitor (or the lack thereof).

1.1.4 Lower mass progenitors and their explosion mechanisms

At the lower end of the progenitor mass range for CCSNe, the SN IIn phenomena may also arise from ecSNe rather than the very high mass stars that become LBVs. In the case of an ecSN, the deflagration of the degenerate core of an 8–10 $M_{\odot}$ star is triggered by electron capture in ^{24}Mg and ^{20}Ne. The resulting explosion is less energetic than regular SNe II, leaving behind a neutron star (Miyaji et al. 1980; Nomoto 1984, 1987). A recent example of an ecSN is SN 2018zd in NGC 2146 (Zhang et al. 2020; Hiramatsu et al. 2021).

Smith (2013) and Moriya et al. (2014) explore the possible link between these lower mass ecSN progenitors and SNe IIn by analysis of the Crab Nebula (M 1), the remnant of the Galactic SN 1054 (Duyvendak 1942; Mayall & Oort 1942). Historical accounts of SN 1054 seem to contradict predictions that an ecSN would be less luminous than a regular SN II, and Moriya et al. (2014) explore CSM interaction as a possible solution to this. In the 8–10 $M_{\odot}$ progenitor mass range, we may find super-AGB stars that undergo mass-loss via massive winds, in turn forming the CSM required for the SN IIn phenomenon. As discussed in Section 1.1.3, a possible progenitor path for SN 2008S-like transients is dust-enshrouded super-AGBs that explode as ecSNe; however, this cannot be confirmed without late-time imaging showing that the progenitor has disappeared. Adams et al. (2016) found that SN 2008S had dimmed to levels below its progenitor, but the dimming of a surviving progenitor can also be explained by extreme dust (dusty environments are typical in SN 2008S-like transients).

SN IIn-like features may be produced by a Type Ia SN detonating within a dense CSM (Deng et al. 2004; Dilday et al. 2012; Silverman et al. 2013). The origin of the CSM is poorly understood. Dilday et al. (2012) investigated the SN Ia-CSM PTF 11kx and found that the progenitor system was a white dwarf (WD) with a red giant or supergiant companion in a symbiotic system. In this particular case, the CSM may have consisted of the material ejected by the giant's wind and perhaps material ejected from previous nova eruptions (see also Wang et al. 2019; Darnley et al. 2019).

SN 2002ic was the first unambiguous detection of an SN Ia-CSM that displayed prominent and persistent multicomponent H α and H β emission lines (Hamuy et al. 2003). A number of SNe IIn have been reclassified as SNe Ia-CSM once their thermonuclear origin became apparent. Their spectrum evolves to show the characteristic broad SN Ia absorption (e.g. Si II) features, but the Balmer emission endures, as in SN 1997cy (Germany et al. 2000; Prieto et al. 2005) and SN 2005gj (Prieto et al. 2005; Aldering et al. 2006). The nature of some SNe Ia-CSM is more ambiguous. Inserra et al. (2016) presented photometric and spectroscopic data spanning 525 d, finding that the spectrum is CSM-interaction dominated throughout all epochs. The authors modelled the ejecta and energetics of the explosion and argued that the CSM mass and energies required to power the light curve are inconsistent with a thermonuclear explosion, instead requiring a CCSN. Out of a sample of six SNe Ia-CSM (SN 1997cy, SN 1999E, SN 2002ic, SN 2005gj, PTF11kx, and SN 2012ca) that the authors compared, only PTF11kx was consistent with the thermonuclear detonation of a WD in dense CSM.

1.2 Environments of SNe IIn

Reflecting the potential diversity in SN IIn progenitors, we see a range of properties in their local environments, particularly in terms of association with SF. As discussed in Section 1.1.1, LBVs are the progenitors of some SNe IIn, but as LBVs are very massive and short-lived one would expect them to be strongly associated with ongoing SF as traced by H α emission.

In order to gauge the association of the location of an SN with H α emission, the pixel statistics technique, normalized cumulative ranking (NCR; James & Anderson 2006; Anderson et al. 2012), is used on continuum-subtracted H α images of SN host galaxies. Anderson & James (2008) found that the SNe IIn in their sample of 12 objects did not trace the H α emission compared to SNe with massive progenitors such as Type Ic SNe. They also found that the SNe IIn more closely followed near-ultraviolet emission, particularly as observed by the *Galaxy Evolution Explorer (GALEX)* space telescope. The isolation of some of these SNe IIn from SF, such as HSC16aayt, may suggest that there could be a small amount of SF being enshrouded by dust (Moriya et al. 2019).

Habergham et al. (2014) used the H α NCR technique on a sample of 17 SNe IIn, finding that the SNe did not follow ongoing SF as traced by H α emission. They concluded that the diversity in the SNe IIn and the diversity in their environments point towards multiple progenitor paths to SNe IIn.

1.3 Motivation for a systematically reclassified target list

There is great variety in the spectral and photometric features of SNe IIn. With this diversity in mind, it is worth noting that spectral classification software packages such as SuperNova IDentification (SNID; Blondin & Tonry 2007) use templates for SN spectral classification. The SN IIn template selection of SNID is limited to three objects: SN 1996L, SN 1997cy, and SN 1998S. Furthermore, SNID has templates over a number of epochs; however, as mentioned earlier, some objects can be classified as an SN IIn at a particular epoch when it may be a gap transient or an SN Ia-CSM, or vice versa. This issue may be exacerbated when the target only has a single spectrum available.

Contamination from the interstellar medium (ISM) or the underlying H II region may influence some classifications if the spectrum has not had an ISM model for that galaxy subtracted. As there is a strong and narrow H α emission feature in the ISM, it can often appear that the broad SN ejecta components have a narrow component superimposed and may seem to represent the H α profile of an SN IIn. This becomes challenging to untangle from the SN data if the spectrum has low resolution and the [N II] lines that lie on either side of the H α line are blended together with the H α emission. Online data bases may retain the SN IIn classification for some of these objects that have no strong evidence of CSM interaction.

The literature describes numerous ways to categorize SNe IIn. Ofek et al. (2014) call SNe IIn that exhibit CSM interaction features for a short period of time (such as PTF 11iqb) 'weak' SNe IIn. SNe IIn typically have spectra that exhibit enduring CSM interaction. Some subcategories are also used such as SN IIn-P and IIn-L, but also SN IId where the narrow H α line has a P Cygni profile, such as in SN 2013gc (Benetti 2000; Reguitti et al. 2019). Furthermore, at later epochs an object may be reclassified (for example, as a standard SN II) and online resources mark the object with the new classification despite the previous evidence of CSM interaction.

The SN IIn subclass was coined by Schlegel (1990). There are a number of pre-1990 SNe that have subsequently been recognized as potential SNe IIn (for example, SN 1978K, SN 1987C, and SN 1989R). However, public data bases may retain the original classification, so when one searches for SNe IIn, the pre-1990 SNe may be missed.

The aim of this study is to provide a systematically reclassified/reconfirmed sample of nearby (within redshift $z < 0.02$) SNe IIn based on simple criteria – the presence of a detectable narrow feature in the H α profile. Section 2 sets out the methodology employed to classify our SN IIn spectra. In Section 3, we present our results and spectral analysis, examine the spectral category breakdown, and show exemplar spectra and H α profile of each category. Our findings are discussed in Section 4.

2 METHODOLOGY

2.1 Collating the sample

An initial catalogue of local SNe IIn (within $z < 0.02$) was constructed from the Open Supernova Catalogue (OSC; Guillochon et al. 2017). As of early 2019, there are 144 SNe that have at some point held an SN IIn classification.[1] All associated spectral data were downloaded from the OSC. There were no data for a number of our objects in the OSC. We also checked the Transient Name Server (TNS).[2] However, for some of the SNe IIn in the catalogue there were no publicly available data. Where the OSC entries provide references for the classifications, we contacted the original observers to request spectral data.

2.2 Classifying the spectra

We present the spectra collected from our archival sources in Section 2. Where available, these are ordered in a time-series plot using `pyplot` (v3.3.3; Hunter 2007) and placed into their rest frame using redshifts from the OSC entries.

As the main defining feature of SN IIn spectra is the multicomponent Balmer emission lines, we focus on the strongest line, H α. We use the PYTHON package `pyspeckit` (v0.1.22; Ginsburg & Mirocha 2011) to fit Gaussians to a multicomponent H α profile, in velocity space.

We begin constructing our H α profile models by fitting a baseline to the continuum. Fitting is restricted to the region around H α (6400–6800 Å). We use the `specfit` routine in `pyspeckit` to fit Gaussians to the spectra. Fits for relatively narrow ($<$1000 km s^{-1}), intermediate ($\sim$1000–2000 km s^{-1}), and broad ($>$5000 km s^{-1}) components are trialled. A reduced χ^2 (calculated, along with uncertainties in the parameters of the fit, by `specfit`) test is used to determine the goodness of fit, which allows us to decide whether a two- or three-component fit is most appropriate by favouring the number of components with the lowest reduced χ^2 value. We propagate the errors in the Gaussian component parameters to calculate the uncertainty of the total fit. False 'IIn' classifications are present in the literature, which seem to arise from the background H II region of the host galaxy contaminating the spectrum, giving an appearance of narrow lines upon a broad feature that originates from the SN itself. To tackle this, we also fit for the nebular [N II] (6584 and 6548 Å) doublet to determine whether any narrow features seen can simply be attributed to H II region pollution rather than to interaction with CSM.

We also include SNe that may show flash-ionization features in our analysis. Flash-spectroscopy SNe exhibit very narrow (usually unresolved) lines that are indicative of CSM ionization for a brief period post explosion (typically $<$10 d) before the SN ejecta sweep up the CSM and the typical SN broad lines dominate the Balmer line profiles thereafter (Khazov et al. 2016). A number of SNe IIn show this brief CSM ionization, such as SN 1998S (Leonard et al. 2000; Shivvers et al. 2015) and PTF 11iqb (Smith et al. 2015). In these cases, CSM interaction was observed at later epochs, so these flash-ionization events cannot be eliminated from our analysis. However, if there are later spectral epochs that show that the transient is a standard SN II, then we do not classify these objects as an SN IIn. We include the SN Ia-CSM subtype as part of the SN IIn class, as the SN IIn phenomenon is an environmental effect rather than being due to the intrinsic properties of the progenitor and explosion.

The FWHM of the Gaussian line profiles allows us to estimate velocities of both the narrow component from the CSM interaction and the broader components from electron scattering and the SN ejecta. For an object to be classified as an SN IIn, the spectrum must have at least a narrow component and either an intermediate-width or broad component. Some of the objects will have narrow, intermediate, and broad components.

Gap-transient (see Section 1.1.3) spectra can be very similar to those of SNe IIn. We check for a peak magnitude (SN 'impostors' typically have a peak $\gtrsim -14$ mag) and the literature to see if a surviving progenitor has been discovered or the object is otherwise a gap transient rather than a full-fledged SN. Similarly, the H α profiles of active galactic nuclei (AGNs) are similar to those of SNe IIn with broad lines from the AGN and narrow lines from the galaxy (Filippenko 1989; Osterbrock & Ferland 2006). Potential AGNs can be ruled out of our sample by looking at whether the SNe are located in the nucleus of the host galaxy; Ward et al. (2021) find that very few AGNs are offset significantly from the nucleus. If an SN is central, we can look for the nebular [O III] $\lambda\lambda$4959, 5007 lines that are found in AGNs; if absent, the object is likely an SN rather than an AGN. We also check the literature to see if any central transients are known to either be an AGN or have been studied as SNe. A decision tree for our classification scheme is shown in Fig. 3.

The now systematically reclassified spectra can be distributed into three categories as follows:

Gold sample: These are SNe IIn that maintain their relatively narrow components throughout their evolution. We require a gold SN IIn to have multiple spectral epochs that span more than $\sim$10 d, which is longer than the typical CSM flash-ionization time-scale. Gold SNe IIn may have the classic 'Eiffel Tower' H α profile or perhaps a more complex structure. These may be further assigned a more specific classification such as SN 1988Z-like or SN 1998S-like. Objects in this gold sample must be surrounded by dense CSM

[1] The object has a cited SN IIn classification, but this may not currently be the primary classification. The object appears in searches for SNe IIn.
[2] https://www.wis-tns.org/ developed by O. Yaron, A. Sass, N. Knezevic, I. Manulis, E. Ofek and A. Gal-Yam.

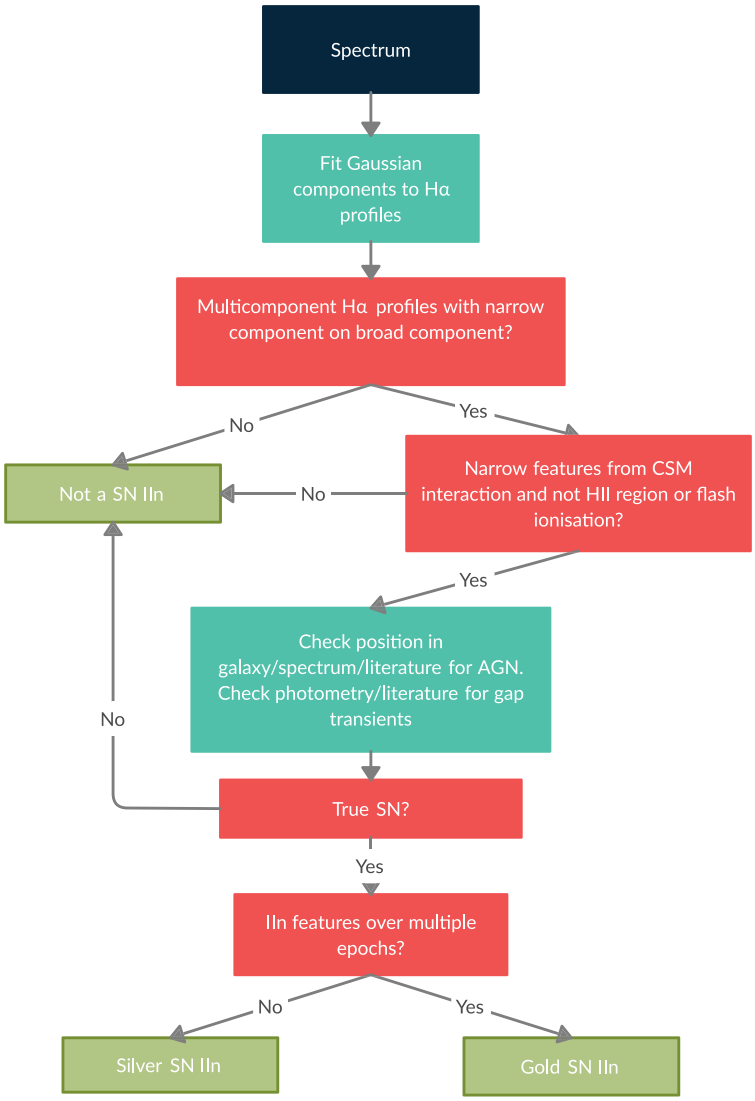

Figure 3. A decision tree describing our classification scheme for the SN IIn spectra.

for there to be sufficient ongoing interaction to maintain the narrow features throughout their spectral evolution.

Silver sample: The silver sample contains SNe with spectra that have some unambiguous narrow features that are consistent with CSM interaction. However, the interaction may not be particularly strong compared to gold-sample objects, and these could be younger transients that have not been monitored spectroscopically. Furthermore, silver-sample objects may not exhibit the narrow interaction features throughout their evolution. An example of a silver-sample object is PTF11iqb, which Smith et al. (2015) remark is an SN IIn that transitions into an SN IIP (an SN IIn-P) and may have had an RSG progenitor similar to those of SNe IIP. PTF 11iqb shows renewed signs of CSM interaction at later times, which Smith et al. (2015) interpret to be the CSM disc re-emerging as the SN photosphere recedes. We also categorize objects with a single spectrum available to us as silver SNe IIn owing to the lack of information regarding the spectral evolution. For a silver SN IIn to be promoted to the gold category, more data are required; many of the silver SNe IIn are in this category owing to there being only a single available spectrum. If there is a single spectrum where the CSM interaction may be consistent with flash ionization, we classify these objects as silver SNe IIn. They can be demoted to not being an SN IIn if the CSM interaction fades and the spectrum resembles a 'standard' SN II.

Not an SN IIn: The spectral data do not show an SN IIn, or were noisy or of otherwise poor quality, and a definitive classification cannot be made positively or negatively. In some cases, the available data do not appear to show an SN spectrum at all, or the available data may not exhibit any SN IIn features. For example, the spectrum may be contaminated by emission from the underlying H II region and the narrow H α feature can be erroneously interpreted as being caused by CSM interaction.

While we do not use them as part of our classification, in order to highlight the ambiguities in SN IIn classification we compare the classifications stated in TNS and OSC to our own reclassifications and also to the results of the template-matching software, SuperNova IDentification (SNID). SNID calculates a quantity, *rlap*, that describes the how well a template is matched to a given spectrum (a full description is given by Blondin & Tonry 2007). The higher the *rlap* value, the better the match. SNID has an *rlap* cut-off of 5, where an *rlap* value <5 indicates a poor match.

Table 1. Breakdown of new categories for our sample of 115 transients.

Category	Number in sample
Gold	37
Silver	50
Not SN IIn	28

3 RESULTS

We obtained usable data for 115 SN IIn candidates either from publicly available data bases or from the original observers. In Table 1, we present the breakdown of how many targets are in each category. We present spectra and H α profile Gaussian fits in Figs 4–13. In Table 2, we outline the reasons some of our transients were classified as not being SNe IIn. Table 3 contains the number of transients that do not have SN IIn primary classifications on the online data bases, OSC and TNS. Finally, Table 4 shows the number of transients that were classified as SNe IIn by SNID. Tables showing the transients we classify into each of our categories can be found in the supplemental online materials.

3.1 SN IIn spectral categories

In this section, we present a selection of spectra from the new SN IIn categories described in Section 2. We show SN spectra and the accompanying H α profiles overlaid with the multi-Gaussian fits for each category.

3.1.1 The gold sample

From the set of 115 SN IIn candidates, we classify 37 as 'gold'. These exhibit unambiguous CSM interaction over numerous epochs.

An example of a gold SN IIn is SN 2008J in MCG-02-7-33, discovered on 2008 January 15 (UT dates are used throughout this paper) with the 0.76 m Katzman Automatic Imaging Telescope (KAIT) as part of the Lick Observatory Supernova Search (Filippenko et al. 2001) at a clear-filter magnitude of 15.4 (Thrasher, Li & Filippenko 2008). Using the *Spitzer Space Telescope*, Fox, Chevalier & Skrutskie (2010) detected late-time near-IR emission at 3.6 and 4.5 μm, which they interpret as emission from warm dust. Fox et al. (2013) did not find late-time CSM interaction in optical spectra obtained with the LRIS and DEIMOS instruments on the Keck 10 m telescopes.

Taddia et al. (2012) present evidence that SN 2008J may be a reddened thermonuclear SN IIn (thus, an SN Ia-CSM) with $A_V \approx$ 1.9 mag. They find that the near-IR light curves and optical spectra of SN 2008J are similar to those of the thermonuclear SNe IIn (or SNe Ia-CSM) SN 2002ic (Hamuy et al. 2003) and SN 2005gj (Prieto et al. 2005). Early-time high-resolution spectra show Na ID λ5891 absorption features and blueshifted Si II λ6355 absorption.

We have 12 epochs of spectral data for SN 2008J shown in Fig. 4. These data cover 311 d throughout which the H α profile retains strong CSM interaction signatures. The first four spectra show Na ID and some Si II absorption (Taddia et al. 2012) and later spectra become noisy. All epochs are fairly featureless or noisy apart from the Balmer lines and the Na ID absorption. Fig. 5 displays the H α profile for the first epoch of SN 2008J. We obtain a good fit to the data from a pair of Gaussian profiles. The broader component has an FWHM of ∼2200 km s^{-1} and the narrow component has an FWHM of ≈400 km s^{-1}. The profile has the classic 'Eiffel Tower' shape. SNID classifies SN 2008J as an SN IIn.

Our second example of a gold-class SN IIn is SN 2009ip in NGC 7259, which was discovered on 2009 August 26 at 17.9 mag by Maza et al. (2009) using the 0.41 m PROMPT-3 telescope at Cerro Tololo Inter-American Observatory. SN 2009ip is notable for being recognized as an SN 'impostor' with a peak of about −13.7 mag (Berger et al. 2009b; Smith et al. 2010). Following this initial eruptive phase, there were phases of rebrightening before a final eruption in 2012 that has been interpreted as a genuine SN IIn (e.g. Mauerhan & Smith 2012; Prieto, Brimacombe & Drake 2012; Pastorello et al. 2013; Margutti et al. 2014; Ofek et al. 2014; Smith 2014) with a peak around −18.3 mag. However, scenarios where the 2012 eruption was non-terminal are discussed in Section 1.1.3.

During the eruptions in the initial 'impostor' phase, it was reported that SN 2009ip may be the result of LBV outbursts (Li et al. 2009a; Miller et al. 2009). Those authors and Nugent (2007) note that archival data from the *HST* and the Palomar Oschin Schmidt telescope reveal a transient coincident with SN 2009ip. This may support the conclusions of Ofek et al. (2014) that there are precursor eruptions to some SNe IIn. Foley et al. (2011) found that there was a possible progenitor identified in archival *HST* data from 1999. Thoene et al. (2015) reported that SN 2009ip had become dimmer than its proposed progenitor by 2015 November 29, which suggests that the 2012 eruption was terminal and SN 2009ip had exploded as a genuine SN.

We present the time-series spectra of SN 2009ip in Fig. 6. 38 spectral epochs spanning 755 d were collected. All epochs show prominent H α emission with the classic SN IIn profile shape. H β is also visible at many of the epochs, and H γ and H δ are seen at earlier epochs along with possible He I λ5876 emission. Apart from these lines, the spectra are featureless. We show the example H α profile at epoch seven of SN 2009ip in Fig. 7. We fit three Gaussian components to this line, with the broader component having an FWHM of ≈5400 km s^{-1}, an intermediate component with an FWHM of ≈1300 km s^{-1}, and the narrow component having an FWHM of ≈300 km s^{-1}. SNID classifies SN 2009ip as either an SN IIP or an AGN (although it most certainly is *not* an AGN).

3.1.2 The silver sample

Our data set contains 50 SNe IIn in the silver category. This category is for objects having spectra that are consistent with SNe IIn but there is only a single spectrum available, or for those where the CSM interaction is short-lived such as in the case of 'weak' SNe IIn.

In Fig. 8, we display the spectrum of the silver SN 2017gas. It was discovered in 2MASX J20171114+5812094 on 2017 August 17 at a *V*-band magnitude of ∼16 as part of the All-Sky Automated Survey for SuperNovae (ASAS-SN) with 14 cm telescopes in Chile and Hawaii (Stanek 2017). We classify SN 2017gas in the silver category because there was only a single spectrum available publicly. It shows very strong CSM interaction features with the 'Eiffel Tower' profile being very apparent in the H α, H β, and H γ emission lines. Furthermore, some non-Balmer lines seem to exhibit the narrow features expected from CSM interaction; we may see narrow features in Fe II λ5750 and Fe II λ5872.

SN 2017gas appears to be close to the centre of 2MASX J20171114+5812094, so we must distinguish this object from an AGN. The host offset of SN 2017gas is 1.97 arcsec (according to PS1; Flewelling et al. 2020), the host has a semimajor axis of 8.80 arcsec, and Skrutskie et al. (2006) report an uncertainty of 0.23 arcsec in the centre of the host right ascension and

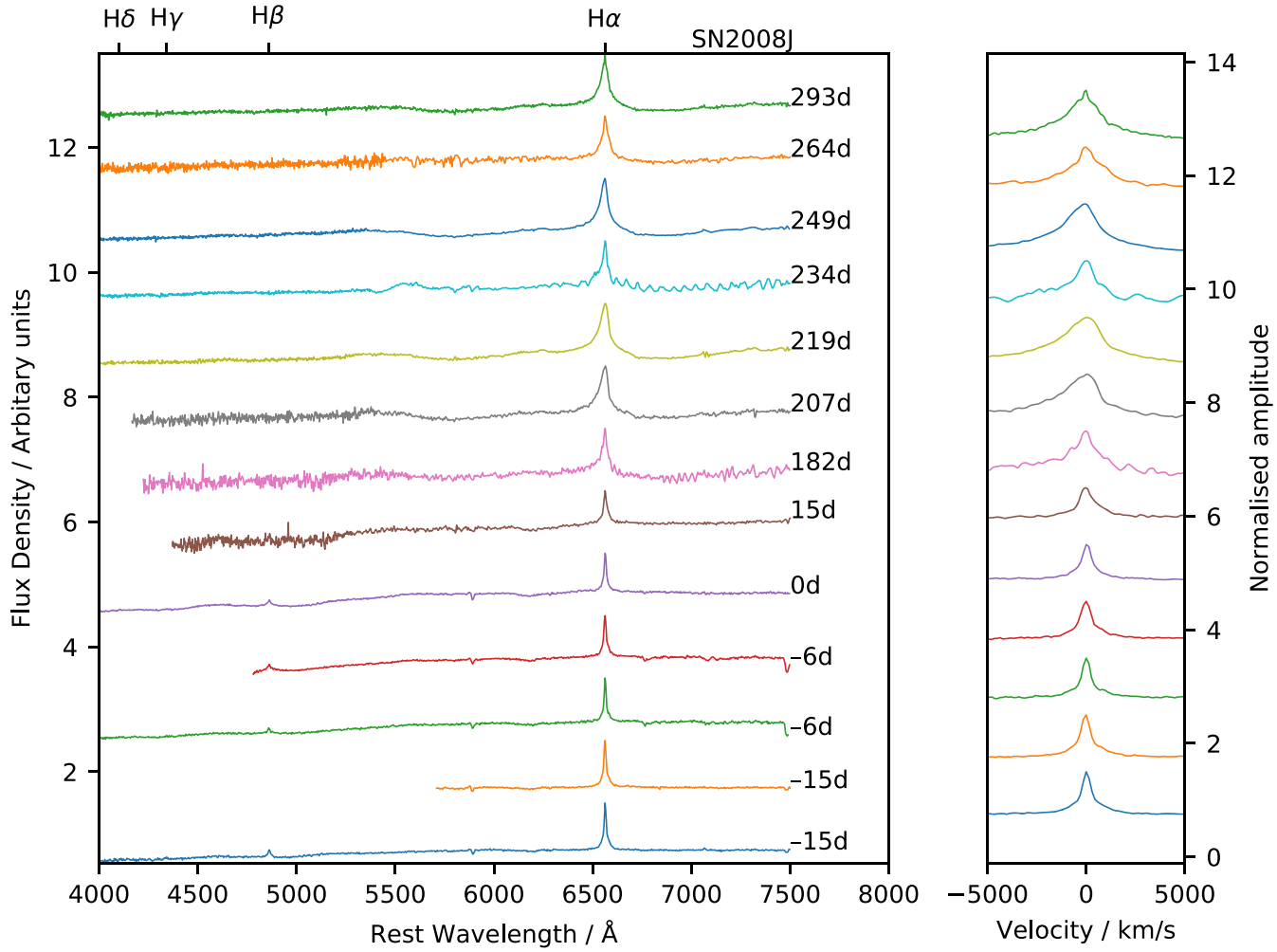

Figure 4. (Left) Time-series spectra of an exemplar SN IIn – SN 2008J. We show optical spectra at 12 epochs over the range 4000–7500 Å that exhibit strong CSM interaction features. Each spectrum is shifted to the rest frame and plotted with a vertical offset, and the Balmer lines from H α through H δ are indicated with tick marks. The numbers are the days after maximum brightness (2008 February 2) in the *i* band. (Right) We plot the corresponding H α profiles in velocity space with a vertical offset for clarity.

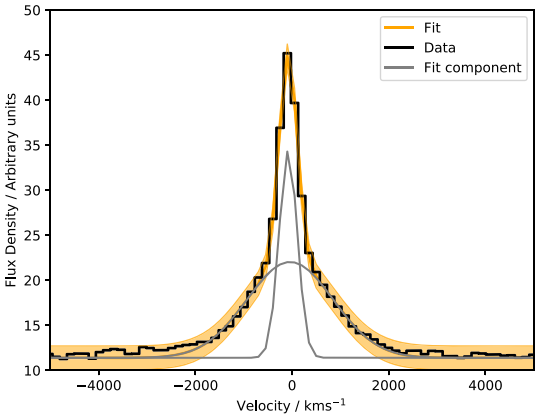

Figure 5. H α profile and the multi-Gaussian fits for the first spectral epoch (15 d before *i*-band maximum) of SN 2008J. We fit a broad component and a narrow component to the data centred around rest-frame H α. The thick black line is the data, the grey lines are the Gaussian components, and the shaded orange area is the total fit along with its 3σ uncertainty region.

declination. Discovery images show the transient being off-centre.[3] The spectrum of SN 2017gas does not show the strong [O III] $\lambda\lambda$4959, 5007 emission lines that may be associated with AGNs. Furthermore, Ward et al. (2021) found that out of a sample of 5493 AGNs, only 9 were offset from the galaxy centre, and the maximum observed offset was 1.649 arcsec $\pm$ 0.004 arcsec. This suggests that the transient is likely an SN rather than an AGN.

The fit to the H α profile of SN 2017gas is shown in Fig. 9. We were able to fit two Gaussians with the FWHM of the broad component being $\sim$1900 km s^{-1} and FWHM $\approx$400 km s^{-1} for the narrow component. SNID matches the spectrum of SN 2017gas to a galaxy template spectrum.

3.1.3 *The non-SN IIn spectra*

There are 28 objects that we classify as not belonging to the SN IIn class. This group includes SNe with spectra that cannot be positively identified as an SN IIn owing to a noisy spectrum, underlying H II

[3] https://star.pst.qub.ac.uk/ps1threepi/psdb/candidate/120171135158120800/

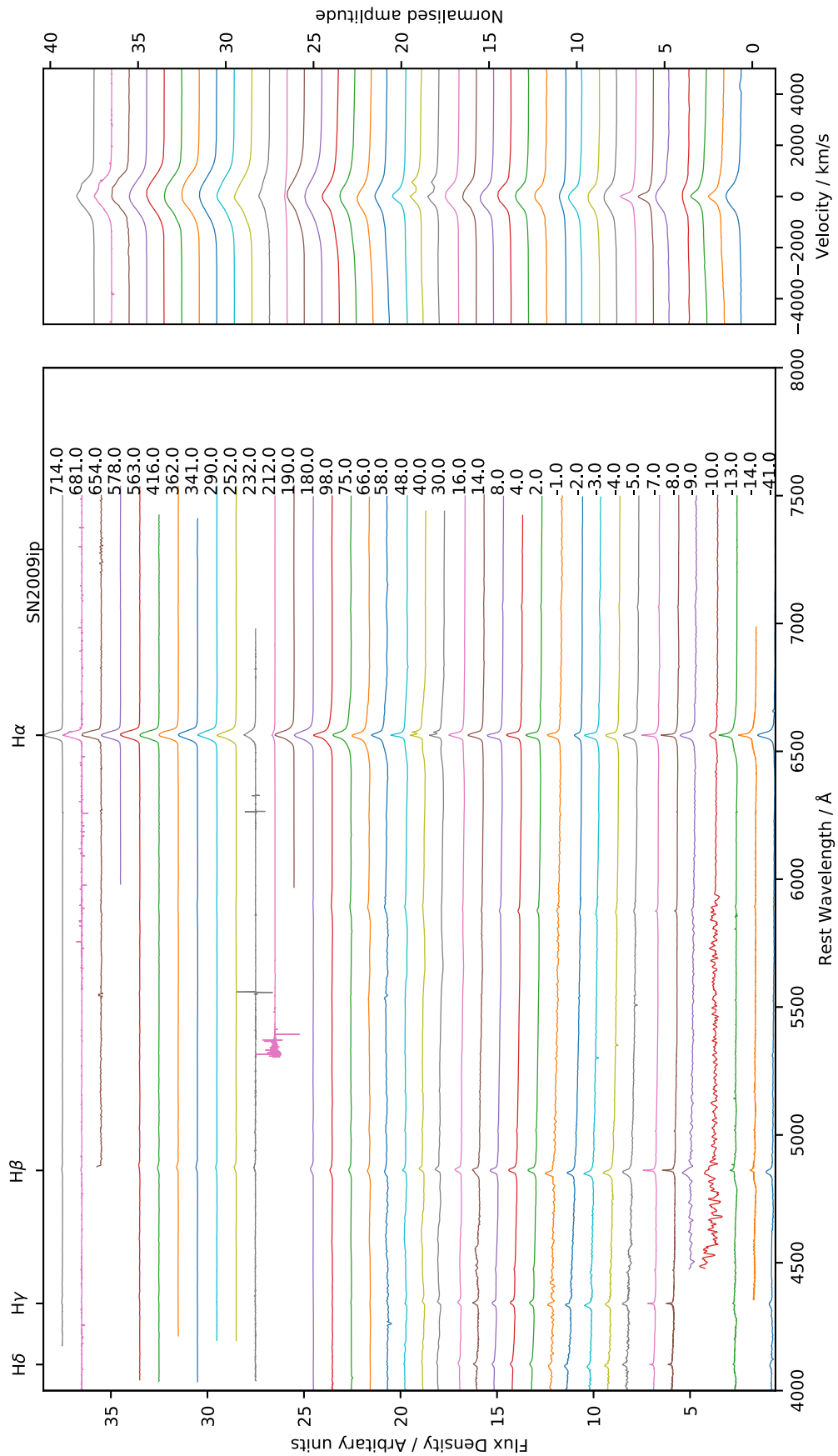

Figure 6. Time-series spectra of an exemplar SN IIn – SN 2009ip in NGC 7259. (*Left*) Spectra spanning 38 epochs over 755 d. The dashed lines mark the Balmer series and there is a vertical offset between each spectrum for clarity. The numbers are the days from maximum brightness (2012 July 24) in the *UVM2* band. (Right) H α profiles of each epoch in velocity space with an offset.

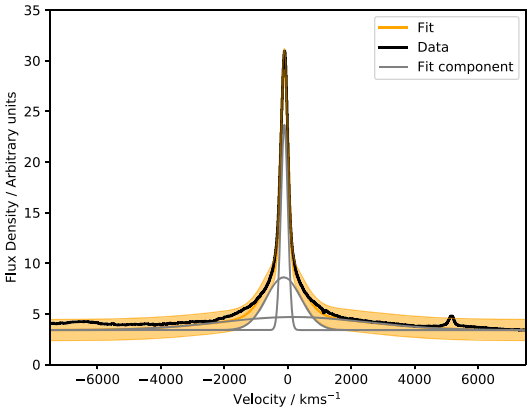

Figure 7. Multicomponent Gaussian fits to epoch seven (7 d before *UVM2*-band maximum) of SN 2009ip. We were able to fit three components to the data: a broad feature, an intermediate-width component, and a narrower component. The thick black line is the data, the grey lines are the Gaussian components, and the shaded orange area is the total fit along with its 3σ uncertainty region.

region pollution, not showing SN-like features or CSM interaction restricted to early times suggesting flash ionization.

An example of a transient that is not an SN IIn is SN 2009kr in NGC 1823. It was discovered on 2009 November 6 with a 0.6 m reflecting telescope at a magnitude of ∼16 (Nakano, Yusa & Kadota 2009). Tendulkar et al. (2009) obtained a spectrum of SN 2009kr with the Palomar 5 m telescope and used SNID to compare with standard templates. They concluded that the apparent prominent narrow feature in the H α emission line indicates that SN 2009kr is an SN IIn. However, Steele, Cobb & Filippenko (2009) analysed spectra of SN 2009kr from the 3 m Shane telescope at Lick Observatory and found that the narrow H α emission component is likely H II region pollution; the prior classification as an SN IIn is due to this and blending of the [N II] lines on either side of H α. They subsequently classify SN 2009kr as an ordinary SN II.

Analysis of images by Elias-Rosa et al. (2010) showed that SN 2009kr may be an SN IIL; however, Fraser et al. (2010) claim that the early-time light curve is more consistent with SN 2009kr being an SN IIP. Elias-Rosa et al. (2010) also found that the progenitor system of SN 2009kr may be a yellow supergiant. Fraser et al. (2010) concluded that the progenitor is ambiguous; if the progenitor was a single star it would be yellow supergiant, but the progenitor could not be ruled out as being in a cluster. The progenitor was quite luminous in *HST* images ($M_I \approx -8.5$ mag). Li et al. (2009b) stated that the progenitor may be in a compact star cluster, and Maund et al. (2015) suggested that the progenitor may be in a compact cluster with a mass of ∼6000 $M_\odot$ after analysis of late-time observations of SN 2009kr.

We display a temporal series of spectra of SN 2009kr in Fig. 10. At early times (the three epochs before maximum brightness), there are narrow Balmer emission lines. A narrow feature superimposed upon the H α line persists over all observed epochs. The post-maximum spectra show a broadening H α line with a P Cygni profile. In Fig. 11, we show the fourth epoch of SN 2009kr (12.4 d post-maximum); this is when the H α emission line starts to broaden with an FWHM of ∼7500 km s^{-1}. We fit narrow features at H α and also [N II] λλ6548, 6584, consistent with the spectrum being contaminated by underlying emission from the local H II region. Furthermore, one can see probable emission features of [S II] λλ6717, 6731, supporting the argument that the narrow features previously interpreted as being due to CSM interaction are actually line pollution from the local ISM. Our analysis is therefore consistent with that of Steele et al. (2009). Despite the evidence that suggests SN 2009kr is not an SN IIn, the OSC has the primary classification of SN 2009kr as an SN IIn. SNID classifies SN 2009kr as an SN IIP.

Another example is SN 2002kg in NGC 2403. SN 2002kg was reported on 2006 October 26 with KAIT as part of LOTOSS (the Lick Observatory and Tenagra Observatory Supernova Search), with a discovery magnitude of ∼19.0 (Schwartz et al. 2003). Subsequent spectroscopic observations were carried out by Filippenko & Chornock (2003) using the Keck Observatory. We show the temporal series of spectra of SN 2002kg in Fig. 12, covering four epochs over 4309 d. Fig. 13 displays the H α profile of SN 2002kg, overlaid with Gaussian fits to the data. The spectra are mostly featureless apart from some Balmer emission and [N II] λλ6548, 6584 lines. SN 2002kg was initially classified as an SN IIn owing to the narrow H α feature (∼300 km s^{-1}) and a possible broader component. However, Filippenko & Chornock (2003) drew comparisons to gap transients such as SN 2000ch (Wagner et al. 2000). They noted that the forbidden nitrogen lines, absence of any other forbidden lines, and an absolute magnitude of about −9 point towards a nitrogen-enriched wind or CSM consistent with the outburst of a massive star such as an LBV rather than an SN. However, these authors did not rule out an SN explosion until there is further evidence that this transient is an 'impostor'.

KAIT photometry, Keck spectroscopy, archival data, and subsequent observations were used to constrain the properties of SN 2002kg. It was found that that the outburst is less energetic than most other 'impostor' events and that the progenitor is the LBV V37 (Tammann & Sandage 1968). It has been reported that the outburst may be forming an LBV nebula, with the eruption being consistent with an S Dor LBV phase and a progenitor mass of 60–80 $M_\odot$ (Weis & Bomans 2005; Maund et al. 2006; Van Dyk et al. 2006; Humphreys et al. 2017). There is no multicomponent H α feature present in the spectra, and the spectra are not at an early stage, so we classify SN 2002kg as not being an SN IIn. SNID classifies SN 2002kg as an AGN (though it certainly was *not* an AGN).

A third example of a transient we do not classify as an SN IIn is SN 2001fa in NGC 673, which was discovered on 2001 October 18 with KAIT as part of LOTOSS, with a discovery magnitude of ∼16.9. Later, a spectrum obtained with the Lick 3 m Shane telescope revealed that SN 2001fa was a young SN IIn that also exhibited WR features including He II, C III, and N III emission lines (Papenkova & Li 2001). There are spectra at 11 epochs spanning 86 d that we present in Fig. 14. The early-time spectra are mostly featureless with the exception of the Balmer lines, in particular H α, as is characteristic of SNe IIn. SN 2001fa exhibited signatures of CSM interaction only visible for ∼5 d and the spectrum subsequently resembled a more standard SN II with a broadened H α profile. There may be a narrow feature on the 10th epoch (0.76 d before maximum brightness), but it could be due to contamination from an H II region. We therefore do not classify SN 2001fa as an SN IIn, as the early-time CSM interaction is representative of flash ionization and later spectra are consistent with those of a standard SN II. Light-curve analysis by Faran et al. (2014) presents SN 2001fa as part of a sample of SNe IIL. SNID classifies SN 2001fa as evolving from an SN IIn to an SN IIP.

Fig. 15 shows the H α profile for the fourth epoch of SN 2001fa. We fit two components to it, with the broad component having an FWHM of ≈1500 km s^{-1} and the narrow component having an FWHM of ≈100 km s^{-1}.

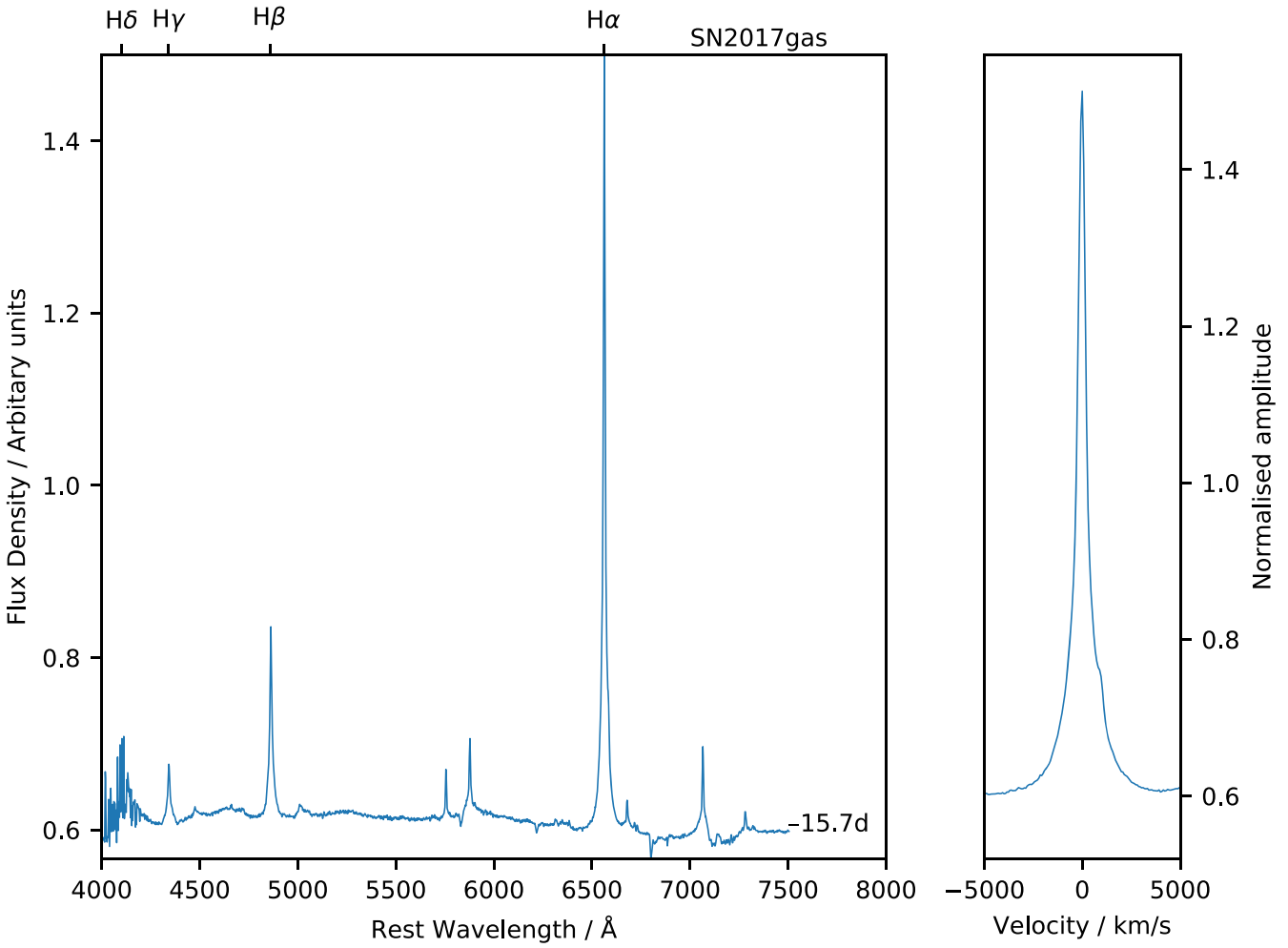

Figure 8. (Left) Spectrum of an exemplar silver class SN IIn – SN 2017gas. We show a single-epoch optical spectrum (15.7 d before maximum brightness in the *R* band on 2017 August 10) over the range 4000–7500 Å that shows strong CSM interaction features. The spectrum is shifted to the rest frame and the Balmer lines are indicated with tick marks. (Right) The corresponding H α profile in velocity space.

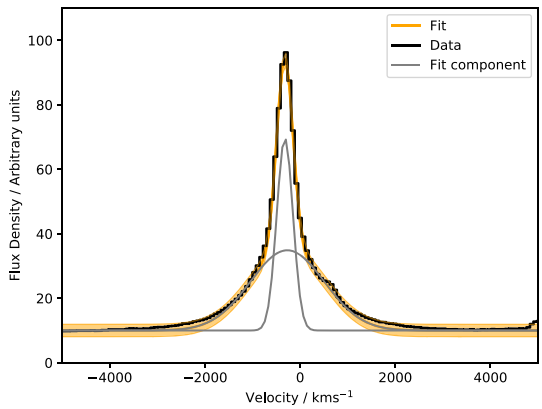

Figure 9. Multicomponent Gaussian fit to the only available spectrum of SN 2017gas. We were able to fit two Gaussian components, one broad and the other narrower. The thick black line is the data, the grey lines are the Gaussian components, and the shaded orange area is the total fit along with its 3σ uncertainty region.

We find that 28 of our objects are not SNe IIn. In Table 2, we show that out of these, 12 may have been misclassified owing to H II region lines being interpreted as CSM interaction. The remaining nine were gap transients that have retained their SN IIn classification in OSC and/or TNS.

3.1.4 Changing classifications

The motivation for this study was to provide a catalogue of systematically reclassified SNe IIn, as the classifications reported in public data bases can be incorrect. We compare our classifications to those recorded as the main class stated by the OSC and the TNS, shown in Table 3. Furthermore, we note that of the 115 SNe in our sample, TNS did not give a classification or spectral data for 12 objects.

3.1.5 SNID results

In Section 4, we present the results of the template matching using SNID. SNID was able to match 32 of our targets to template SNe IIn. In the instances where there was no match to an SN IIn spectrum, we

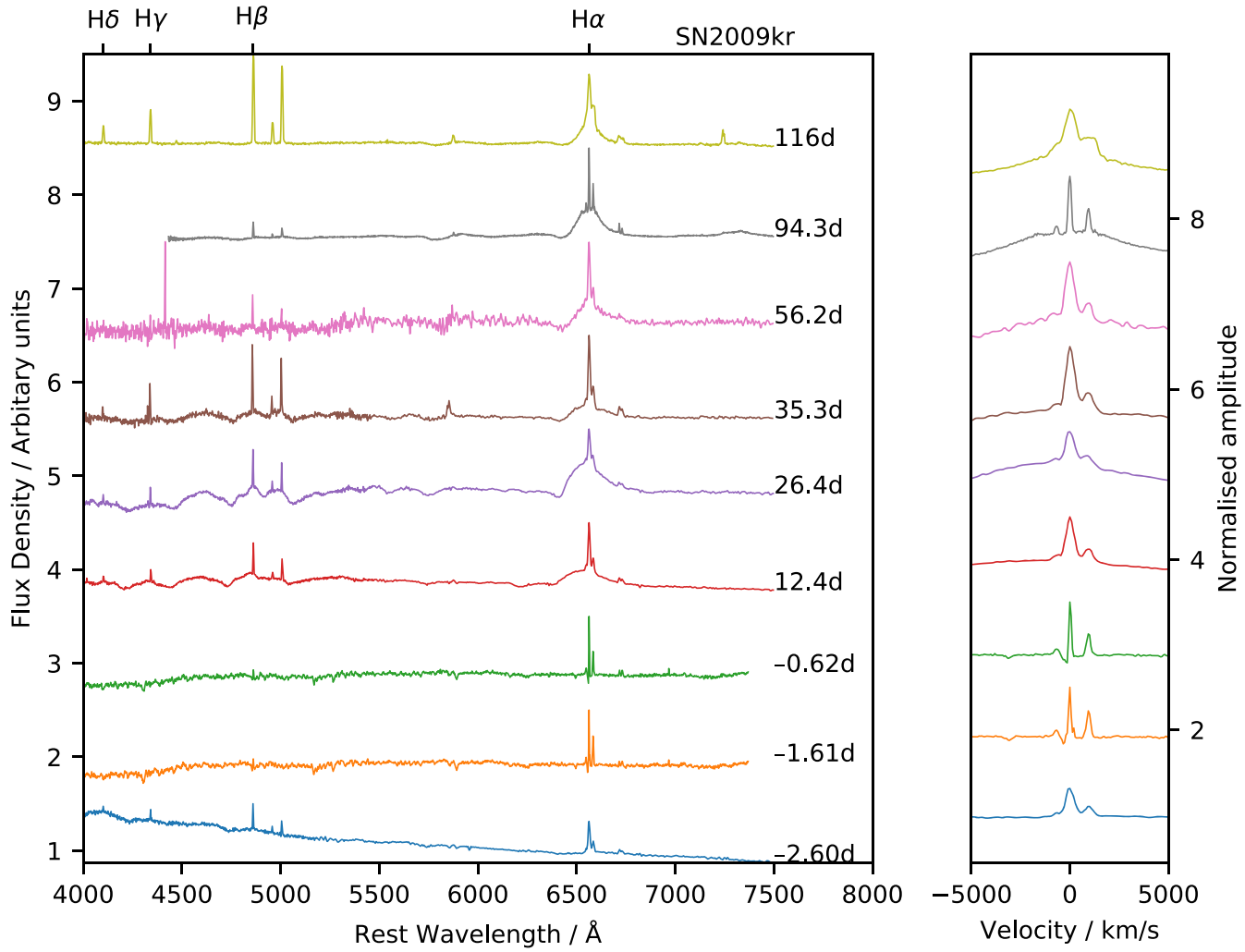

Figure 10. Temporal series of spectra of an example non-SN IIn classification – SN 2009kr. We display optical spectra over the range 4000–7500 Å at nine epochs, showing that the previously claimed CSM interaction features are likely due to the spectra being polluted by emission lines from the underlying H II region; the [N II] lines on either side of H α and the [S II] lines redward of H α are clearly visible at all epochs. This object therefore may be a standard SN II rather than an SN IIn. Each spectrum is shifted to the rest frame, a vertical offset is added for clarity, and the Balmer series from H α through H δ is indicated with tick marks. The numbers on the right of the spectra denote the days from maximum brightness (2009 November 6) in the *K* band. (Right) Corresponding H α profiles in velocity space, with vertical offsets.

note that there are 26 matches to AGN spectra and 39 have matches to other SN classes. We find that 18 match galaxy spectra and 5 match the spectra of LBV templates. We also find that six of our objects have spectra that evolve into/out of the SN IIn subclass according to SNID.

4 DISCUSSION AND SUMMARY

In this work, we have explored the spectral diversity in the SN IIn subclass. We spectroscopically reclassified 115 objects within $z < 0.02$ that have at some point been classified as an SN IIn in the OSC. The main result is that 40 per cent of the SNe in our sample had been misclassified when one takes account of the primary classification in OSC. Furthermore, ∼25 per cent of the objects in our sample are not SNe IIn when considering our classification scheme. Moreover, for objects that are not SNe IIn, 11 or 18 (OSC or TNS, respectively) claim a primary SN IIn classification. We also find that there is disagreement in the classification for 45 per cent of our sample between the OSC and TNS. Therefore, any work based on such catalogues of SNe IIn could have included SNe that are misclassified or miss some targets.

This disagreement is clearly problematic for work that relies on samples and catalogues of SNe. Our work was initiated when it was noticed that when an individual SN was searched in data bases, the claimed class may differ between data bases and also changes in the OSC depending on search parameters. Without our reclassification, the SN IIn catalogue would contain at least 28 targets that do not appear to be SNe IIn, possibly leading to erroneous conclusions in subsequent studies. Confusion in the classification of SNe IIn may come from a number of sources that contribute to the diversity in the SN IIn subclass.

As described in Section 1, some of this diversity may be explained by considering multiple progenitor paths. The proposed progenitors of SNe IIn often quoted in the literature are LBVs. The environmental analysis of Habergham et al. (2014) shows that the SF environments of SNe IIn are not consistent with high-mass LBVs as the sole progenitor path, suggesting that there may be lower mass progenitor routes. Further to this, the stellar-evolution models of Maeder &

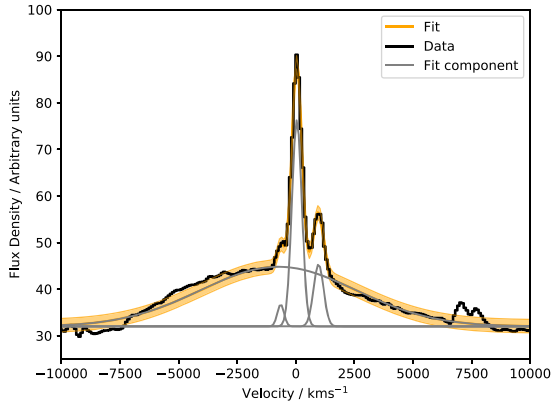

Figure 11. Multicomponent Gaussian fits to the fourth epoch of SN 2009kr just over 12 d past maximum brightness in the *K* band. We were able to fit a broad component to the H α profile along with three narrow components at H α and [N II] $\lambda\lambda$6548, 6584. The [S II] $\lambda\lambda$6717, 6731 lines are also visible. The presence of these lines indicates that the narrow features seen in this H α profile probably originate from the underlying H II region. The thick black line is the data, the grey lines are the Gaussian components, and the shaded orange area is the total fit along with its 3σ uncertainty region.

Meynet (2008) show that LBVs must become WR stars before an SN eruption, and some examples from our sample (such as SN 2001fa) show WR lines in their spectra. However, Groh, Georgy & Ekström (2013) find that when a rotational component is added to evolution models, LBVs may terminate in an SN explosion without requiring a WR phase.

The mass-loss mechanism of LBVs is poorly constrained. Dwarkadas (2011) find that previous assumptions regarding the LBV mass-loss rate being constant may be flawed, as this does not account for the density of CSM required for the SN IIn-like features to be apparent. Instead, the mass-loss mechanism may be episodic eruptions preceding the SN, and the progenitor may have transitioned to a WR star by the time the SN occurs. This is consistent with Ofek et al. (2014), who find that mass-loss events that cause brightening are common in SN IIn progenitors; they are seen in around half of a sample of SNe IIn observed by PTF. Furthermore, Strotjohann et al. (2021) find that month-long precursor events brighter than an absolute magnitude of −13 were found in ∼25 per cent of a sample of 131 SNe IIn from ZTF within the three months prior to the SN explosion.

As well as this single-star route to LBVs, there are proposed binary-evolution paths for LBVs or LBV-like objects. Sana et al. (2012) found that most massive stars evolve in binary systems (∼70 per cent of the O-type stars in their sample were in a binary). Smith & Tombleson (2015) showed that LBVs are often isolated, away from regions of ongoing SF. As discussed in Section 1.1.1, this may be due to the stars being kicked from their original cluster through interactions with companions or stellar mergers (Justham et al. 2014; Aghakhanloo et al. 2017).

Since the CSM interaction that causes the SN IIn phenomenon is an environmental effect, we include SNe IIn that may be SNe Ia-CSM or flash-ionization SNe in our analysis; they might be counted in the lower mass progenitor channel, or in the case of the flash-ionization SNe not be SNe IIn at all. In our sample, it is possible that some of the silver SNe IIn may show short-lived flash-ionization behaviour where the progenitor undergoes mass-loss shortly before the SN explosion, creating a confined CSM shell (Khazov et al. 2016). For example, SN 2007cm may exhibit a flash-ionization spectrum on day 0, when there is an SN IIn-like H α profile, but by day 15 this narrow feature has faded and the spectrum represents a fairly standard SN II spectrum. When there are data to show the transition to a standard SN II, we do not classify it as an SN IIn. Khazov et al. (2016) have the 'weak' SN IIn PTF 11iqb in their sample of flash-ionization SNe. While many flash-ionization SNe evolve into standard SNe II with no subsequent CSM interaction (Bruch et al. 2021), others exhibit CSM interaction at later times, such as PTF 11iqb (Smith et al. 2015). Moreover, this flash-ionization phase is similar to the spectra of many young SN IIn, with a mostly featureless continuum and narrow CSM interaction signatures on the H α emission line. We therefore cannot rule out young SNe with single spectral epochs; they are classified in the silver category. The CSM around SNe IIn is complex, and in order to better understand the nature of these objects, longer term observations are needed to determine whether CSM interaction re-emerges. These weaker SNe IIn may indicate that the mass-loss required for the SN IIn-like features has a continuum starting from 'normal' SN progenitors such as RSGs, rather than being exclusive to the massive LBVs. SNe that are classified at early times may be classified as SNe IIn owing to flash-ionization features that endure for ∼10 d post-explosion. Without follow-up data there may be a number of misclassifications, as some of these SNe might evolve into 'standard' SNe II.

To be able to promote a silver-class object to the gold class, follow-up observations are required. The silver-class SNe IIn with a single spectrum and young SNe IIn with no immediate follow-up data may show strong CSM interaction over multiple epochs and be promoted to the gold category if subsequent observations indicate ongoing interaction. The SN may have short-lived CSM interaction at later times and be more like the proposed SN IIn-L or SN IIn-P subclasses. Additional observations of the objects that we did not classify as SNe IIn may reduce uncertainty in their classification if the H II regions were omitted from the spectra. Observations of the H II regions in the host galaxies could be utilized to create templates that can be subtracted from the spectra to remove the contamination, and then CSM interaction features would become clearer if present. Conversely, if the only CSM interaction shown is fleeting and at early times (i.e. flash ionization), with the spectrum then evolving into a standard SN II, we can demote a silver SN IIn to not being an SN IIn. We demoted three such transients in this study: SN 2001fa, SN 2007cm, and SN 2014G.

Follow-up observations are the key to add clarity to the SN IIn classifications. Current transient surveys such as ZTF find enormous numbers of transients with thousands of SNe discovered each year (Feindt et al. 2019), and the Vera Rubin Observatory (formerly the Large Synoptic Survey Telescope; LSST Science Collaboration 2009) might discover ∼10^5 SNe per year. While this may be advantageous for catching the early-time flash spectra, prompt follow-up observations of enormous numbers of transients will be challenging. Such data are particularly important for gap transients. Suspected SN 'impostors' may be dust-obscured SNe leading to a substantially reduced observed brightness, so a gap transient actually being a fully fledged SN cannot always be ruled out. Late-time observations of gap transients can confirm the survival of the progenitor. An example of a debated gap transient is SN 2008S, which is often used as a prototypical SN 'impostor'; however, Adams et al. (2016) suggest that extreme dust behaviour must be invoked to account for a star surviving while SN 2008S became dimmer than its progenitor. Conversely, as discussed in Section 1.1.3, some transients such as the final eruption of SN 2009ip may be interpreted as a terminal CCSN explosion (Pastorello et al. 2013; Smith et al. 2014), but this is disputed (Fraser et al. 2013, 2015). Non-terminal eruptions cannot

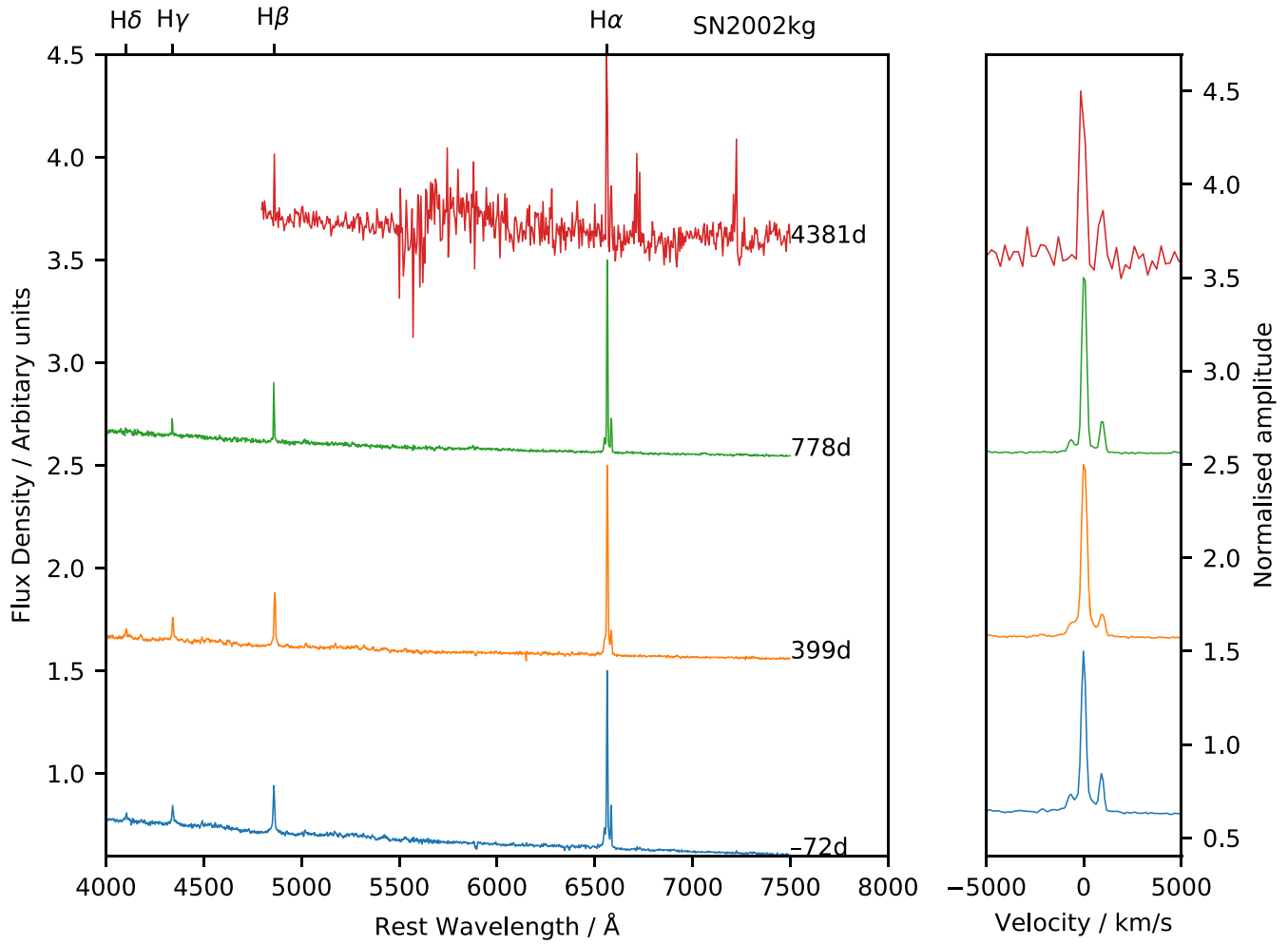

Figure 12. Time-series spectra of an example of a negative SN IIn classification – SN 2002kg. We show optical spectra from 4000–7500 Å over four epochs that are mostly featureless apart from Balmer emission and [N II]. The H α line is strong and narrow and the H β line is also apparent in these spectra. Each epoch is shifted to the rest frame, an offset is added for clarity, and the Balmer series from H δ–H α is marked with a tick. The numbers are the days from maximum (2002 October 26) in the Clear band. (Right) Corresponding H α profiles in velocity space with offsets.

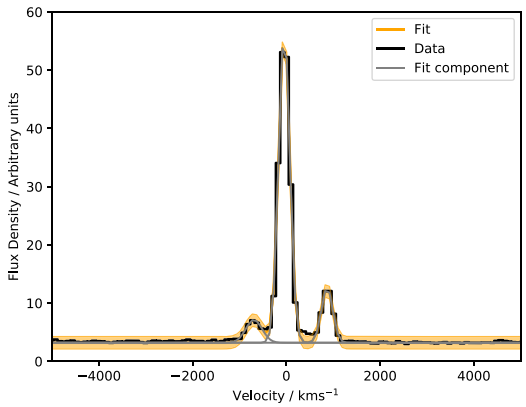

Figure 13. Multicomponent Gaussian fits to the H α profile of the third epoch (778 d post maximum brightness in the Clear band) of SN 2002kg. We fit a narrow H α profile with an FWHM of $\approx$300 km s^{-1}. [N II] lines are also visible and may indicate that SN 2002kg is an SN 'impostor' where the transient is the brightening of an LBV due to a mass-loss event. The thick black line is the data, the grey lines are the Gaussian components, and the shaded orange area is the total fit along with its 3σ uncertainty region.

be ruled out until late-time observations can confirm the survival or death of the progenitor.

In our group of SNe that are not reclassified as SNe IIn, the gap transients such as SN 2002kg have primary classifications as SNe IIn in OSC or TNS. As previously discussed, in the case of SN 2002kg, Schwartz et al. (2003) recognize that SN 2002kg may be an 'impostor' but hold an SN IIn classification until further evidence of a non-terminal explosion is revealed. Van Dyk et al. (2006) found that the photometric and spectroscopic properties of SN 2002kg represent LBV outbursts in the S Dor phase. Weis & Bomans (2005) found that the position of SN 2002kg in Isaac Newton Telescope (INT) observations was coincident with the LBV NGC 2403-V37; however, the classifications in the public data bases were not updated to reflect the new evidence.

In Section 1, we described the classic 'Eiffel Tower' H α profile of SNe IIn. The actual H α profile may deviate from the classic profile, possibly complicating efforts to classify the object. The standard symmetrical SN IIn profile is formed from a spherical shell of H-rich CSM, but Dwarkadas (2011) find that a clump of CSM is sufficient to create SN IIn-like features. Indeed, there seems to be a variety of H α profile shapes observed that may result from the CSM having a variety of different geometries, with the inclination to the line of

Table 2. Objects that are not SNe IIn and the reasons for classifications.

Name	Reason for a not SN IIn classification
SN 2001dk	Consistent with H II region contamination
SN 2001fa	Flash-ionization SN
SN 2004F	Consistent with H II region contamination
SN 2001I	Consistent with H II region contamination
SN 2002bj	Consistent with H II region contamination
SN 2009kr	Consistent with H II region contamination
SN 2004gd	Consistent with H II region contamination
SN 2002kg	Gap transient
SN 1999gb	Consistent with H II region contamination
SN 2010al	Consistent with H II region contamination
SN 2002an	No narrow feature
SN 2003ke	Consistent with H II region contamination
SN 1999bw	Gap transient
SN 2000ch	Gap transient
SN 2014G	Flash-ionization SN
SN 2001ac	Gap transient
SN 1997bs	Gap transient
SN 2002bu	Gap transient
SN 2017jfs	Gap transient
SN 2006bv	Gap transient
SN 2007cm	Flash-ionization SN
SN 2001dc	No narrow feature
ASASSN-15hs	Consistent with H II region contamination
SN 2013by	Consistent with H II region contamination
SN 2001ad	No narrow feature
SN 2018dfy	Consistent with H II region contamination
SN 2006fp	Gap transient
SN 2008gm	Consistent with H II region contamination

Table 3. Breakdown of the number of objects in the OSC and TNS having non-SN IIn primary classifications (out of 115) and the number of occurrences where the OSC and TNS disagree on the primary classification.

Class	OSC	TNS	Disagreement
Gold	16	6	16
Silver	18	6	18
Not an SN IIn	16	10	15

Table 4. Results of using SNID to match the spectral data to templates. In total, SNID matched 32 of our 115 targets to SN IIn templates.

Class	SNID IIn matches
Gold	15 out of 37
Silver	14 out of 50
Not SN IIn	3 out of 28

sight also having an effect. Harvey et al. (2020) shows how different shell morphologies can affect line profiles. An example of a deviation from a symmetrical profile is shown in the middle spectral epochs of SN 2009ip (Fig. 6), where there may be a double-peaked H α profile, and at later epochs a 'hump' appears on the red side of the profile. A further example of this profile diversity is the proposed subclass SN IId (Benetti 2000); examples of SNe IId within our catalogue may include SN 2009kn and SN 2013gc (Reguitti et al. 2019). There are signs of an aspherical CSM exhibited by SN 1998S (Leonard et al. 2000), and the CSM may be contained in a disc around PTF 11iqb (Smith et al. 2015).

4.1 SN 1978K and other caveats

We have chosen a simple classification scheme that only relies on the Balmer line profiles. This allows our classifications to be independent of the complexities and heterogeneity of SN IIn spectra. However, there are a small number of objects that do not fit into this regime but are an important consideration.

SN 1978K in NGC 1313 was discovered in 1990 by Dopita & Ryder (1990) and was initially classified as a classical nova system. Subsequent observations of NGC 1313 found that this 'nova' was both a strong radio and X-ray source (Schlegel et al. 1999). Archival photographic plates reveal a dim, possibly dust-enshrouded SN at the 'nova' location in mid-1978 and the object was designated SN 1978K (Chapman et al. 1992). A spectrum was taken over 13 000 d post-eruption (Chugai, Danziger & della Valle 1995). The narrow H α line has an FWHM of $\sim$500 km s^{-1}. Ryder et al. (1993) observed SN 1978K at optical, X-ray, and radio wavelengths, and propose that the ongoing emission from the SN remnant may be explained by SN ejecta interacting with a dense shell of CSM. Kuncarayakti et al. (2016) made observations of SN 1978K with the Very Large Telescope and found that the CSM interaction is ongoing over 35 yr post-explosion. Furthermore, SNID matches the spectrum of SN 1978K to the template spectrum of SN 1996L 322 d post-explosion.

Very early time SN IIn spectra may exhibit a strong blue continuum but no broad component in the H α profile, yet showing narrow H α emission (Filippenko 1997). In the case of SN 1978K, the broad SN ejecta components have faded, leaving only the relatively narrow lines from ongoing CSM interaction. Therefore, it is important to consider the age of the spectrum. This is not always possible, however, as observation dates are not recorded on public data bases in every instance.

As discussed previously, caution must be taken to ensure that gap transients and AGNs do not infiltrate the SN IIn sample, since their H α profiles can be similar (Filippenko 1989). We did not identify any AGNs in our sample, but after comparing peak magnitudes and searching the literature we find that nine of our objects are gap transients. One of these transients, SN 2017jfs (also known as AT 2017jfs), has an SN IIn-like spectrum and was initially classified as an SN IIn, but photometric and spectroscopic analysis revealed that this transient was a luminous red nova (Pastorello et al. 2019a).

Our classification scheme may miss late-time CSM interaction that does not conform with the 'Eiffel Tower' H α profile shape. We do not classify SN 2014G as an SN IIn, since the apparent CSM interaction features were seen only at early times and thus indicative of flash ionization. Terreran et al. (2016) found that SN 2014G photometrically behaved as an SN IIL, but at $\sim$100 d post-maximum luminosity, the spectrum started forming a feature on the blue side of H α. This feature grew over time along with the [O I] $\lambda\lambda$6300, 6363 doublet. The authors interpreted this unusual feature as late-time interaction with a highly asymmetric CSM. As our classification scheme is localized to the H α region, we would not consider this possible CSM interaction feature.

4.2 SNID and H II region contamination

Most of the objects that are not SNe IIn were initially categorized as SNe IIn owing to contamination from the underlying H II regions. These H II region features include narrow H α and [N II] $\lambda\lambda$6548, 6584 lines. If these lines are not considered, it is possible that the narrow features on top of the broad SN H α emission could be

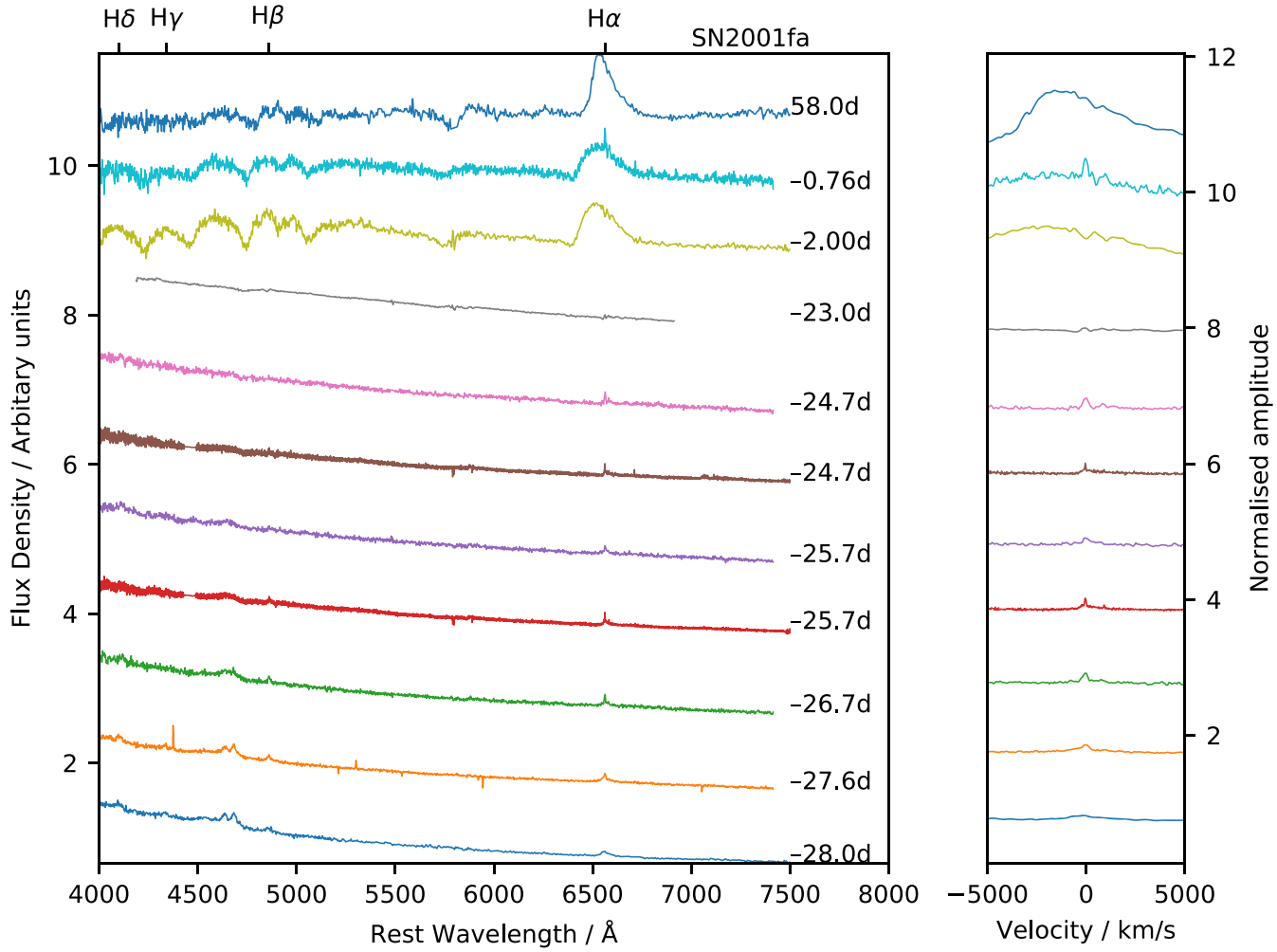

Figure 14. Time series of spectra of an exemplar silver-class SN IIn – SN 2001fa. We display optical spectra over the range 4000–7500 Å at nine epochs that show CSM interaction features at earlier times, followed by more-standard SN II characteristics with broad H α emission and possible P Cygni features in several lines. Each spectrum is shifted to the rest frame, a vertical offset is added for clarity, and the Balmer series from H α through H δ is indicated with tick marks. The numbers are the days from maximum (2001 November 17) in the Clear band. (Right) Corresponding H α profiles in velocity space, with vertical offsets.

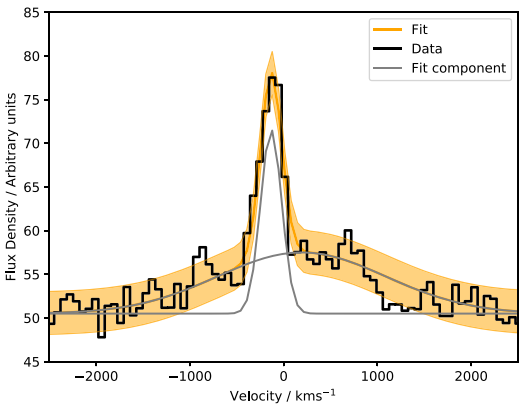

Figure 15. Multicomponent Gaussian fits to the fourth epoch (25.7 d before maximum brightness in the Clear band) of SN 2001fa. We were able to fit two Gaussian components to the data, one intermediate-broad and the other narrow. The thick black line is the data, the grey lines are the Gaussian components, and the shaded orange area is the total fit along with its 3σ uncertainty region.

misinterpreted as signatures of CSM interaction, hence leading to an erroneous classification of SN IIn. An example of an SN with such H II contamination that has a primary classification of SN IIn in online data bases is SN 2009kr (see Fig. 10). This SN has multiple spectral epochs with consistent H II contamination. Moreover, Steele et al. (2009) point out the H II contamination of SN 2009kr, but the object still retains a primary SN IIn classification in OSC. This highlights the importance of keeping transient entries on public data bases up to date, to reflect new data. In cases where there may be H II region contamination superimposed upon an H α profile that shows genuine CSM interaction, our classification scheme could be applied to H β where the relatively narrow features and intermediate-width components may be present (Filippenko 1997).

Template-matching routines such as SNID are a popular tool for the classification of SN spectra. These routines rely on templates of archetypal members of a spectral class. The heterogeneity found in SN IIn spectra may cause issues with such template-matching methods that have a limited number of templates for less-common SN classes. This is apparent when we find that only 32 of our targets (all from the gold and silver groups) were matched to an SN IIn template

by SNID (see Table 4). In the case of SN 'impostors', photometric data or late-time observations are required to differentiate an object as a gap transient rather than an SN IIn. Similarly, SNID classifies 23 objects in our sample as AGNs, but we do not identify any genuine AGNs in our sample, as none lie near the centre of their host galaxy and also show the characteristic nebular [O III] λλ4959, 5007 lines.

For the SNe with H II region pollution, if a spectrum has low resolution ($R \lesssim 500$), or if a noisy spectrum is heavily binned, it is possible that the [N II] lines blend with H α to make an illusion of an SN IIn-like profile. Spectroscopic templates of the gold SNe IIn will be produced in the hope of increasing the sample of reference templates to better reflect the great diversity we see in SNe IIn.

This study has relied on the collection of data from public sources such as OSC and from the original classifiers. However, data from the public data bases often have little metadata available, with the spectra files in the ASCII format. For example, these spectra frequently lack information about the observer, the telescope or instrument, and in some cases even the exact date of observation. While the OSC quotes times in terms of days from maximum brightness, the band in which the maximum is observed may be IR rather than optical, so quoted times may not correspond well to the time of explosion. There are also many unpublished spectra that further complicate any studies wishing to use large SN IIn samples. We were unable to obtain data for 28 objects. While TNS is missing classifications for 12 of the objects, it has fewer misclassifications when compared to OSC, with 12 primary classifications in the gold and silver groups not being an SN IIn compared to the 34 for OSC.

4.3 Summary

We have outlined a simple classification scheme for SNe IIn that takes advantage of their characteristic H α profile and applied this to a sample of 115 SN IIn candidates at $z < 0.02$ that have publicly available data or data that we were able to collect from the original observers. Our sample is based on a catalogue collected for an environmental survey of SNe IIn, and candidates outside of this sample (e.g. at a higher redshift) are beyond the scope of this project. Here, we briefly summarize our key findings and recommendations for future work.

(i) We compiled a catalogue of 115 reclassified transients that have at some point held an SN IIn classification.

(ii) 87 of the 115 SNe have been reconfirmed to be SNe IIn based on their multicomponent H α profile.

(iii) There are 37 gold- and 50 silver-category spectra.

(iv) Gold SNe IIn exhibit CSM interaction over multiple epochs. Silver-category transients are consistent with SNe IIn, but they may have short-lived CSM interaction in the case of transitional objects (e.g. when the classification evolves from SN IIn to SN IIP), or they have quite limited data. Silver SNe IIn can be promoted to gold SNe IIn with more data from follow-up observations. Objects can also be demoted if it becomes apparent that the CSM interaction features are due to flash ionization.

(v) We do not classify 28 SNe as SNe IIn. In most cases, H II region lines contaminate the spectrum and were interpreted as CSM interaction, gap transients, or are consistent with flash ionization.

(vi) 34 of the SNe IIn have a primary classification from the OSC that is not an SN IIn, and TNS has 12 such cases.

(vii) OSC reports that 11 of the targets we classified as not being SNe IIn are SNe IIn, and TNS reports 18 such cases.

(viii) The public data bases OSC and TNS disagree on the classification of 51 of our objects; however, TNS primary classifications seem more reliable, despite lacking classifications for 12 objects.

(ix) SNID classifies 15 out of 37 gold SNe IIn as SNe IIn, and 14 out of 50 silver SNe IIn as SNe IIn. SNID classifies the three SNe with early narrow components that disappear over time, consistent with flash-ionization signatures, as SNe IIn.

(x) Inconsistencies and ambiguities in the classification of SNe IIn may be due to the great range in properties that SNe IIn exhibit. The heterogeneity in the spectral features is perhaps a result of multiple progenitor paths and different environments.

To solidify classifications of SNe IIn, follow-up observations are vital. They provide information on the evolution of the spectra, allowing estimations of the duration of CSM interaction. Furthermore, when an SN IIn classification is found to be erroneous, it is important that the new data are reflected in public data bases, particularly in cases where specific SNe have been studied in depth in the literature. Our classification scheme should be applied to a larger sample of SN IIn candidates, since the current catalogue is limited. We will produce a set of template spectra from the gold category to increase the template selection in SNID to improve classifications in the future. Our SN IIn classifications will be integrated into an ongoing survey of SN IIn environments.

ACKNOWLEDGEMENTS

We would like to thank the referee for their thorough review that provided constructive comments. CLR acknowledges a PhD studentship from the UK Science and Technology Facilities Council (STFC). SMH-M and MJD acknowledge partial funding from STFC. AVF is grateful for funding from the TABASGO Foundation, the Christopher J. Redlich Fund, and the U.C. Berkeley Miller Institute for Basic Research in Science (where he is a Senior Miller Fellow). We would like to thank F. Bauer, N. Blagorodnova, T.G. Brink, P. Challis, N. Elias-Rosa, A. Gal-Yam, M. Hamuy, A. Pastorello, the Padova Classification Program,[4, 5] A. Reguitti, and J. Zhang for providing spectral data used in this work.

Research at Lick Observatory is partially supported by a generous gift from Google. Some of the data presented herein were obtained at the W. M. Keck Observatory, which is operated as a scientific partnership among the California Institute of Technology, the University of California, and The National Aeronautics and Space Administration (NASA); the Observatory was made possible by the generous financial support of the W. M. Keck Foundation.

DATA AVAILABILITY

The data used in this work will be shared upon reasonable request to the author.

REFERENCES

Adams S. M., Kochanek C. S., Prieto J. L., Dai X., Shappee B. J., Stanek K. Z., 2016, MNRAS, 460, 1645
Aghakhanloo M., Murphy J. W., Smith N., Hložek R., 2017, MNRAS, 472, 591
Akashi M., Kashi A., 2020, MNRAS, 494, 3186
Aldering G. et al., 2006, ApJ, 650, 510

[4] https://sngroup.oapd.inaf.it/asiago_class.html
[5] Data used for SN 2011ir (Tomasella et al. 2014).

Anderson J. P., James P. A., 2008, MNRAS, 390, 1527
Anderson J. P., Habergham S. M., James P. A., Hamuy M., 2012, MNRAS, 424, 1372
Anderson J. P. et al., 2014, ApJ, 786, 67
Andrews J. E. et al., 2020, preprint (arXiv:2009.13541)
Arbour R., 2008, Cent. Bur. Electron. Telegrams, 1235, 2
Benetti S., 2000, Mem. Soc. Astron. Ital., 71, 323
Berger E. et al., 2009a, ApJ, 699, 1850
Berger E., Foley R., Ivans I., 2009b, Astron. Telegram, 2184, 1
Bevan A. M. et al., 2020, ApJ, 894, 111
Blanc N. et al., 2005a, Astron. Telegram, 570, 1
Blanc N. et al., 2005b, Astron. Telegram, 630, 1
Blondin S., Tonry J. L., 2007, ApJ, 666, 1024
Boian I., Groh J. H., 2018, A&A, 617, A115
Bond H. E., Bedin L. R., Bonanos A. Z., Humphreys R. M., Monard L. A. G. B., Prieto J. L., Walter F. M., 2009, ApJ, 695, L154
Bostroem K. A. et al., 2019, MNRAS, 485, 5120
Botticella M. T. et al., 2009, MNRAS, 398, 1041
Brennan S. J. et al., 2021a, preprint (arXiv:2102.09572)
Brennan S. J. et al., 2021b, preprint (arXiv:2102.09576)
Bruch R. J. et al., 2021, ApJ, 912, 46
Bullivant C. et al., 2018, MNRAS, 476, 1497
Chapman J. M., Norris R. P., Reynolds J. E., te Lintel Hekkert P., 1992, IAU Circ., 5616, 2
Chugai N. N., 1991, MNRAS, 250, 513
Chugai N. N., 2001, MNRAS, 326, 1448
Chugai N. N., Danziger I. J., della Valle M., 1995, MNRAS, 276, 530
Chugai N. N. et al., 2004, MNRAS, 352, 1213
Darnley M. J. et al., 2019, Nature, 565, 460
de Jager C., 1998, A&AR, 8, 145
Deng J. et al., 2004, ApJ, 605, L37
Dessart L., Hillier D. J., Gezari S., Basa S., Matheson T., 2009, MNRAS, 394, 21
Dilday B. et al., 2012, Science, 337, 942
Dopita M. A., Ryder S. D., 1990, IAU Circ., 4950, 3
Duyvendak J. J. L., 1942, PASP, 54, 91
Dwarkadas V. V., 2011, MNRAS, 412, 1639
Elias-Rosa N. et al., 2010, ApJ, 714, L254
Elias-Rosa N. et al., 2018, MNRAS, 475, 2614
Faran T. et al., 2014, MNRAS, 445, 554
Feindt U., Nordin J., Rigault M., Brinnel V., Dhawan S., Goobar A., Kowalski M., 2019, J. Cosmol. Astropart. Phys., 2019, 005
Filippenko A. V., 1989, AJ, 97, 726
Filippenko A. V., 1997, ARA&A, 35, 309
Filippenko A. V., Chornock R., 2003, IAU Circ., 8051, 2
Filippenko A. V., Li W. D., Treffers R. R., Modjaz M., 2001, in Paczynski B., Chen W.-P., Lemme C., eds, ASP Conf. Ser. Vol. 246, IAU Colloq. 183: Small Telescope Astronomy on Global Scales. Astron. Soc. Pac., San Francisco, p. 121
Flewelling H. A. et al., 2020, ApJS, 251, 7
Foley R. J., Berger E., Fox O., Levesque E. M., Challis P. J., Ivans I. I., Rhoads J. E., Soderberg A. M., 2011, ApJ, 732, 32
Fox O. D., Chevalier R. A., Skrutskie M. F., 2010, Astron. Telegram, 2665, 1
Fox O. D., Filippenko A. V., Skrutskie M. F., Silverman J. M., Ganeshalingam M., Cenko S. B., Clubb K. I., 2013, AJ, 146, 2
Fox O. D. et al., 2015, MNRAS, 454, 4366
Fox O. D. et al., 2020, MNRAS, 498, 517
Fraser M. et al., 2010, ApJ, 714, L280
Fraser M. et al., 2013, MNRAS, 433, 1312
Fraser M. et al., 2015, MNRAS, 453, 3886
Gal-Yam A., Leonard D. C., 2009, Nature, 458, 865
Gal-Yam A. et al., 2007, ApJ, 656, 372
Germany L. M., Reiss D. J., Sadler E. M., Schmidt B. P., Stubbs C. W., 2000, ApJ, 533, 320
Ginsburg A., Mirocha J., 2011, Astrophysics Source Code Library, record ascl:1109.001
Groh J. H., Georgy C., Ekström S., 2013, A&A, 558, L1
Guillochon J., Parrent J., Kelley L. Z., Margutti R., 2017, ApJ, 835, 64
Habergham S. M., Anderson J. P., James P. A., Lyman J. D., 2014, MNRAS, 441, 2230
Hamuy M., 2003, ApJ, 582, 905
Hamuy M., Maza J., 2003, IAU Circ., 8045, 2
Hamuy M., Phillips M., Suntzeff N., Maza J., 2003, IAU Circ., 8151, 2
Harvey E. J. et al., 2020, MNRAS, 499, 2959
Hiramatsu D. et al., 2021, Nature Astron., in press
Huang C., Chevalier R. A., 2018, MNRAS, 475, 1261
Humphreys R. M., Davidson K., 1994, PASP, 106, 1025
Humphreys R. M., Davidson K., Jones T. J., Pogge R. W., Grammer S. H., Prieto J. L., Pritchard T. A., 2012, ApJ, 760, 93
Humphreys R. M., Davidson K., Gordon M. S., Weis K., Burggraf B., Bomans D. J., Martin J. C., 2014, ApJ, 782, L21
Humphreys R. M., Davidson K., Van Dyk S. D., Gordon M. S., 2017, ApJ, 848, 86
Hunter J. D., 2007, Comput. Sci. Eng., 9, 90
Inserra C. et al., 2016, MNRAS, 459, 2721
James P. A., Anderson J. P., 2006, A&A, 453, 57
Justham S., Podsiadlowski P., Vink J. S., 2014, ApJ, 796, 121
Kasliwal M. M., 2011, PhD thesis, California Inst. Technol.
Khazov D. et al., 2016, ApJ, 818, 3
Kiewe M. et al., 2012, ApJ, 744, 10
Kochanek C. S., 2011, ApJ, 741, 37
Kochanek C. S., Szczygieł D. M., Stanek K. Z., 2012, ApJ, 758, 142
Kuncarayakti H., Maeda K., Anderson J. P., Hamuy M., Nomoto K., Galbany L., Doi M., 2016, MNRAS, 458, 2063
Kurfürst P., Pejcha O., Krtička J., 2020, A&A, 642, A214
Leonard D. C., Filippenko A. V., Barth A. J., Matheson T., 2000, ApJ, 536, 239
Li W., Smith N., Miller A. A., Filippenko A. V., 2009a, Astron. Telegram, 2212, 1
Li W., Filippenko A. V., Miller A. A., Cuillandre J. C., Elias-Rosa N., van Dyk S. D., 2009b, Astron. Telegram, 2312, 1
Li W. et al., 2011, MNRAS, 412, 1441
LSST Science Collaboration, 2009, preprint (arXiv:0912.0201)
Maeder A., Meynet G., 2008, in de Koter A., Smith L. J., Waters L. B. F. M., eds, ASP Conf. Ser. Vol. 388, Mass Loss from Stars and the Evolution of Stellar Clusters. Astron. Soc. Pac., San Francisco, p. 3
Margutti R. et al., 2014, ApJ, 780, 21
Mauerhan J., Smith N., 2012, MNRAS, 424, 2659
Mauerhan J. C. et al., 2013, MNRAS, 430, 1801
Maund J. R. et al., 2006, MNRAS, 369, 390
Maund J. R., Fraser M., Reilly E., Ergon M., Mattila S., 2015, MNRAS, 447, 3207
Mayall N. U., Oort J. H., 1942, PASP, 54, 95
Maza J. et al., 2009, Cent. Bur. Electron. Telegrams, 1928, 1
Miller A. A., Li W., Nugent P. E., Bloom J. S., Filippenko A. V., Merritt A. T., 2009, Astron. Telegram, 2183, 1
Millour F. et al., 2020, preprint (arXiv:2006.15660)
Miyaji S., Nomoto K., Yokoi K., Sugimoto D., 1980, PASJ, 32, 303
Modjaz M., Li W. D., Garnavich P., Jha S., Challis P., Kirshner R., Berlind P., 1999, IAU Circ., 7268, 1
Moriya T. J., Blinnikov S. I., Tominaga N., Yoshida N., Tanaka M., Maeda K., Nomoto K., 2012, MNRAS, 428, 1020
Moriya T. J., Maeda K., Taddia F., Sollerman J., Blinnikov S. I., Sorokina E. I., 2014, MNRAS, 439, 2917
Moriya T. J. et al., 2019, ApJ, 882, 70
Moriya T. J. et al., 2020, A&A, 641, A148
Nakano S., Yusa T., Kadota K., 2009, Cent. Bur. Electron. Telegrams, 2006, 1
Nomoto K., 1984, ApJ, 277, 791
Nomoto K., 1987, ApJ, 322, 206
Nugent P., 2007, Astron. Telegram, 1213, 1
Nyholm A. et al., 2020, A&A, 637, A73
Ofek E. O. et al., 2014, ApJ, 789, 104
Osterbrock D. E., Ferland G. J., 2006, Astrophysics of Gaseous Nebulae and Active Galactic Nuclei. Univ. Sci. Books, Sausalito, CA
Papenkova M., Li W. D., 2001, IAU Circ., 7737, 1

Pastorello A. et al., 2007, Nature, 447, 829
Pastorello A. et al., 2013, ApJ, 767, 1
Pastorello A. et al., 2017, MNRAS, 474, 197
Pastorello A. et al., 2019a, A&A, 625, L8
Pastorello A. et al., 2019b, A&A, 628, A93
Prieto J., Garnavich P., Depoy D., Marshall J., Eastman J., Frank S., 2005, Cent. Bur. Electron. Telegrams, 302, 1
Prieto J. L. et al., 2008, ApJ, 681, L9
Prieto J. L., Brimacombe J., Drake A. J., 2012, Astron. Telegram, 4439, 1
Reguitti A. et al., 2019, MNRAS, 482, 2750
Ryder S., Staveley-Smith L., Dopita M., Petre R., Colbert E., Malin D., Schlegel E., 1993, ApJ, 416, 167
Sana H. et al., 2012, Science, 337, 444
Sanders N. E. et al., 2015, ApJ, 799, 208
Schlegel E. M., 1990, MNRAS, 244, 269
Schlegel E. M., Ryder S., Staveley-Smith L., Petre R., Colbert E., Dopita M., Campbell-Wilson D., 1999, AJ, 118, 2689
Schwartz M., Li W., Filippenko A. V., Chornock R., 2003, IAU Circ., 8051, 1
Shivvers I., Groh J. H., Mauerhan J. C., Fox O. D., Leonard D. C., Filippenko A. V., 2015, ApJ, 806, 213
Silverman J. M. et al., 2013, ApJS, 207, 3
Skrutskie M. F. et al., 2006, AJ, 131, 1163
Smith N., 2006, ApJ, 644, 1151
Smith N., 2013, MNRAS, 434, 102
Smith N., 2014, ARA&A, 52, 487
Smith N., Andrews J. E., 2020, MNRAS, 499, 3544
Smith N., Hartigan P., 2006, ApJ, 638, 1045
Smith N., Tombleson R., 2015, MNRAS, 447, 598
Smith N., Gehrz R. D., Hinz P. M., Hoffmann W. F., Hora J. L., Mamajek E. E., Meyer M. R., 2003, AJ, 125, 1458
Smith N. et al., 2007, ApJ, 666, 1116
Smith N. et al., 2009, ApJ, 697, L49
Smith N. et al., 2010, AJ, 139, 1451
Smith N., Li W., Silverman J. M., Ganeshalingam M., Filippenko A. V., 2011, MNRAS, 415, 773
Smith N., Mauerhan J. C., Kasliwal M. M., Burgasser A. J., 2013, MNRAS, 434, 2721
Smith N., Mauerhan J. C., Prieto J. L., 2014, MNRAS, 438, 1191
Smith N. et al., 2015, MNRAS, 449, 1876
Smith N. et al., 2016, MNRAS, 458, 950
Smith N. et al., 2017, MNRAS, 466, 3021
Smith N. et al., 2018, MNRAS, 480, 1466
Stanek K. Z., 2017, Transient Name Server Discovery Report, No. 2017-862
Steele T. N., Cobb B., Filippenko A. V., 2009, Cent. Bur. Electron. Telegrams, 2011, 1
Stritzinger M., Folatelli G., Morrell N., 2008, Cent. Bur. Electron. Telegrams, 1218, 1
Stritzinger M. et al., 2012, ApJ, 756, 173
Strotjohann N. L. et al., 2021, ApJ, 907, 99
Taddia F. et al., 2012, A&A, 545, L7
Taddia F. et al., 2013, A&A, 555, A10
Tammann G. A., Sandage A., 1968, ApJ, 151, 825
Tendulkar S. P., Kasliwal M. M., Quimby R., Kulkarni S. R., 2009, Astron. Telegram, 2291, 1
Terreran G. et al., 2016, MNRAS, 462, 137
Thoene C., de Ugarte Postigo A., Leloudas G., Cano Z., Maeda K., 2015, Astron. Telegram, 8417, 1
Thompson T. A., Prieto J. L., Stanek K. Z., Kistler M. D., Beacom J. F., Kochanek C. S., 2009, ApJ, 705, 1364
Thöne C. C. et al., 2017, A&A, 599, A129
Thrasher P., Li W., Filippenko A. V., 2008, Cent. Bur. Electron. Telegrams, 1211, 1
Tomasella L. et al., 2014, Astron. Nachr., 335, 841
Valenti S. et al., 2016, MNRAS, 459, 3939
Van Dyk S. D., Li W., Filippenko A. V., Humphreys R. M., Chornock R., Foley R., Challis P. M., 2006, preprint (arXiv:astro-ph/0603025)
Vink J. S., 2018, A&A, 619, A54
Wagner R. M. et al., 2000, American Astronomical Society Meeting Abstracts, 44.13
Wang X., Chen J., Wang L., Hu M., Xi G., Yang Y., Zhao X., Li W., 2019, ApJ, 882, 120
Ward C. et al., 2021, ApJ, 913, 102
Weis K., Bomans D. J., 2005, A&A, 429, L13
Weis K., Bomans D. J., 2020, Galaxies, 8, 20
Zhang J. et al., 2020, MNRAS, 498, 84

SUPPORTING INFORMATION

Supplementary data are available at *MNRAS* online.

Table A1. The sample of SNe IIn that were reclassified into the 'gold' spectral category.
Table A2. The sample of SNe IIn that were reclassified into the 'silver' spectral category.
Table A3. The sample of SNe IIn that were reclassified as not being SNe IIn.
Table A4. The sample of SNe IIn for which we were unable to obtain any data.

Please note: Oxford University Press is not responsible for the content or functionality of any supporting materials supplied by the authors. Any queries (other than missing material) should be directed to the corresponding author for the article.

APPENDIX A: CLASSIFICATION TABLES

Here, we present tables containing our sample of SNe organized into their new spectral classifications. Table A1 lists the SNe IIn in the gold category. Tables showing the full lists showing transients in each new classification are shown in the supplementary online materials.

Table A1. The sample of SNe IIn that were reclassified into the 'gold' spectral category. From our sample of 115 transients within $z < 0.02$ with data, 37 SNe are classified as 'gold' SNe IIn where the CSM interaction is visible throughout multiple epochs. The table gives the common SN name, the discovery date, the common host name, the J2000 coordinates, and the redshift. The full version of this table is available online.

Name	Disc. date	Host name	R.A.	Dec.	z	OSC	TNS	SNID	Class	Source
SN2005db	2005/07/19	NGC 214	00:41:26.79	25:29:51.60	0.0151	IIn	IIn	Gal	Gold IIn	Blanc et al. (2005a)
SN2005gl	2005/10/05	NGC 266	00:49:50.02	32:16:56.80	0.0155	IIn	IIn	IIn	Gold IIn	Blanc et al. (2005b)
SN1999eb	1999/10/02	NGC 664	01:43:45.45	04:13:25.90	0.0180	II	IIn	AGN	Gold IIn	Modjaz et al. (1999)
SN2003G	2003/01/08	IC 208	02:08:28.13	06:23:51.90	0.0120	IIn	IIn	AGN	Gold IIn	Hamuy & Maza (2003)
SN2008J	2008/01/15	MCG -02-07-33	02:34:24.20	− 10:50:38.50	0.0159	Ia	IIn	IIn	Gold IIn	Stritzinger, Folatelli & Morrell (2008)
...	...	...	...	...	...	...	...	...	...	...

This paper has been typeset from a TEX/LATEX file prepared by the author.